To the Graduate Council:

I am submitting herewith a thesis written by Benjamin Michael Lamie entitled "Comparative Properties of Polymers Guiding the Development of an Abdominal Aorta Model". I have examined the final paper copy of this thesis for form and content and recommend that it be accepted in partial fulfillment of the requirements for the degree of Masters of Science, with a major in Engineering Science.

Richard Jendrucko

Richard Jendrucko, Major Professor

We have read this thesis
and recommend its approval:

Jack Wasserman

Jack Wasserman

Mehran Kasra

Mehran Kasra

Accepted for the Council:

Vice Chancellor and
Dean of Graduate Studies

Comparative Properties of Polymers Guiding the Development of an Abdominal Aorta Model

A Thesis
Presented for
Master of Science Degree
The University of Tennessee, Knoxville

Benjamin Michael Lamie
December 2005

Dedication

This thesis is dedicated to my very loving and supportive parents Mike Lamie and Cathy Butler, my stepparents Keith Butler and Robin Lamie, my amazing girlfriend Stephanie Hargrove, my maternal grandparents Virginia Booth and the late F.D. Booth, my paternal grandparents Betty Lamie and the late Jim Lamie, my sisters Julie Collins, Alex Lamie, and Emily Lamie, my close personal friends Aaron Fannin, Britt Easter, and Cliff Townsend, and to my mentor and major professor Dr. Richard Jendrucko.

"*And whether we shall meet again I know not. Therefore my everlasting farewell take. If we do meet again, why, we shall smile; if not, then this parting was well made*"
– William Shakespeare

Acknowledgements

First and foremost, I want to convey my deepest appreciation to my family. To my parents Mike Lamie and Cathy Butler, I am who I am today because of you and could not possibly imagine where I would be without your love and support. To my stepparents Keith Butler and Robin Lamie, through the good and the bad we have made it work and I owe as much to you as anyone else. To my beautiful, loving and strong sister Julie Collins, there is and always will be the strongest of bonds between us that constantly keeps you in my thoughts. To my precious sisters Alex and Emily Lamie, you are truly a blessing in my life. To my grandmothers Betty Lamie and Virginia Booth, I want to thank you for going out of you way all of my life to make certain I was taken care of. To my grandfathers the late Jim Lamie and the late F.D. Booth, not a day goes by that I don't think of them and all they taught me. Finally, to my extraordinary, beautiful, intelligent, and loving girlfriend Stephanie Hargrove, what you have done to my life can only be cheapened by my inadequacies as a writer. I can only offer my sincerest gratitude for loving me through all that we have experienced.

I would like to thank my mentor and major professor Dr. Richard Jendrucko. Thanks for your advisement and assistance throughout this project. Thanks for all your support over the last four and a half years I have been at the University of Tennessee and for helping me reach my goals. I would also like to thank Dr. Kasra and Dr. Wasserman, not only for being on my graduate committee but also for all of the knowledge that I have gained from you classes over the last four and a half years.

Throughout the course of this project I received a tremendous amount of assistance and would like to extend my deepest appreciation to the following people. To Dr. Joseph Weigel, thank you for the canine artery specimens that you provided for my testing. This project would not have been possible otherwise. To Mr. Van Branston at the Textile and Nonwovens Development Center (TANDEC) facility, thank you for allowing me to run my tests in your laboratory. Your assistance and experience were vital to a successful testing procedure. To Mark Morrison, thank you for helping me conduct my tests on the artery specimens. I could not have completed my testing without your willingness to help. To Gary To and Drew Herron, thank you for you help on the CAD drawings. The drawings presented would not have been possible otherwise.

Abstract

Hemodynamics, the study of the forces involved in the circulation of blood, is an area that researchers have approached in various manners for many years. The study of how blood flows through arteries and veins as well as the effect of the composition of the blood has been defined and thoroughly characterized in past studies. Although in-depth studies have been performed on the flow characteristics of blood, most often the observations are made as the fluid flows through tubes composed of some rigid material. It is well known that the arteries and veins have a layered histology that show varying viscoelastic characteristics. It is also accepted that the varying geometry of the vessel wall and the taper of the vessel have a significant effect on the flow characteristics of the vascular system. Therefore, a physical model of the vascular system that takes into account the elasticity and varying geometry of the blood vessel would prove extremely valuable in the hemodynamic study of the vascular system.

This study approached the task of determining the most suitable material to incorporate into a physical model of the abdominal aorta. The purpose of this study was to compare the mechanical properties of selected materials to those of canine blood vessels in order to choose which of these materials most accurately represents the viscoelasticity seen in large blood vessels such as the aorta. An in-depth approach to choosing a material with similar mechanical properties is defined. There is also a comparison of the time dependency of the vessel properties as well as the differences of the mechanical properties when the testing is performed in different directions.

The result of this study was the selection of a base material to which modifications will be made in the future to more accurately represent the mechanical properties of the abdominal aorta. It was determined that the time of storage and direction of testing had no effect on the properties demonstrated by the canine thoracic aortas and therefore did not effect the material selection process. The material selection process led to the conclusion that silicone rubber has the most similar mechanical properties to the blood vessels tested and therefore should be incorporated as the base material in a physical model of the abdominal aorta. The future of this study will include expanded testing that includes a broader range of materials and more in depth testing methods such as biaxial tensile tests and creep tests.

Contents

1. Background **1**

1.1 Introduction 1

1.2 Overview of the Human Aorta 2

1.2.1 Structure 2

1.2.2 Branching of the Abdominal Aorta 3

1.2.3 Arterial Wall Structure 4

1.3 Mechanical Behavior of Arterial Tissue 6

1.3.1 Behavior under Uniaxial Loading 6

1.3.2 Collagen Properties 8

1.3.3 Elastin Properties 9

1.3.4 Arterial Tissue Mechanical Properties 9

1.3.5 Mathematical Representation of
Stress-Strain Relationship 11

1.4 Summary of Previous Studies 12

2. Materials and Methods **17**

2.1 Candidate Materials for Arterial Model Study 17

2.1.1 Plastics 18

2.1.2 Elastomers 19

2.1.3 Canine Blood Vessels 20

2.2 Experimental Methods 21

2.2.1 Apparatus 21

2.2.2 Candidate Material Preparation 22

2.2.3 Vessel Preparation 23

2.2.4 Testing Procedure 25

2.2.5 Statistical Analysis 27

3. Results and Discussion **29**

3.1 Overview of Results 29

3.1.1 Time Dependency of Experimental Data 29

3.1.2 Directional Dependency of Experimental Data 31

3.1.3 Candidate Material/Blood Vessel Comparison (Longitudinal) 33
3.1.4 Candidate Material/Blood Vessel Comparison (Circumferential) 35
3.2 Discussion 37
3.2.1 Time Dependency of Arterial Tissue Properties 37
3.2.2 Directional Dependency of Arterial Tissue Properties 40
3.2.3 Material Selection for Abdominal Aorta Models 42
4. Conclusions and Recommendations 47
4.1 Conclusions 47
4.2 Recommendations for Future Work 49
Bibliography 51
Appendix 57
A Model Specifications 59
B Preliminary Ideas for Future Model Development 62
C Statistical Analysis 65
D Calculation of the Taper Factor of the Abdominal Aorta 68
Vita 69

List of Tables

1.1 Mass % Tissue Composition of Arterial Layers 6

2.1 Mechanical Properties of Candidate Materials 18

2.2 Candidate Material Test Specimen Dimensions 23

2.3 Blood Vessel Test Specimen Dimensions 24

3.1 Mechanical Properties Derived from Experimental Data 30

3.2 Results of the Statistical t-Test for Longitudinal Values ($p \leq 0.01$) 32

3.3 Results of the Statistical t-Test of for Circumferential Values ($p \leq 0.01$) 36

A1 Dimensions for Design of Aorta Model 59

List of Figures

1.1 Diagram of the Aorta including the Ascending Aorta, Aortic Arch, and the Thoracic Aorta (Gray 1985) 3

1.2 Arterial Layers (Spence and Mason 1987) 5

2.1 Instron 1122 Model Tensile Tester 22

2.2 Vessels Prepared for Testing 25

2.3 Standard Testing Rates Specified in ASTM Standard 882 26

3.1 Stress-Strain Results (One Day/One Week) 38

3.2 Stress-Strain Results (One Day/One Month) 39

3.3 Stress –Strain Results (Circumferential/Longitudinal/Fung[1997]) 41

3.4 Stress-Strain Results (Plastic) 43

3.5 Stress-Strain Results (Elastomers) 44

3.6 Stress-Strain Results (Silicone Rubber) 45

A1 Change in Anatomical Area along the Abdominal Aorta 60

A2 Computer-Aided Model Drawings 61

C1 Statistical Comparison: Time Dependency 65

C2 Statistical Comparison: Longitudinal Sample 66

C3 Statistical Comparison: Circumferential Sample 67

Chapter 1

Background

1.1 Introduction

Hemodynamics is the study of the forces and resulting flows involved in the circulation of blood in the vascular tree. Continuing studies have led to an in-depth understanding of the forces caused by flow especially at the fluid-vessel wall interface. Such studies have contributed to the understanding of the way conditions such as atherosclerosis and congenital heart failure affect blood flow and how they are treated. Although many in-vitro studies have been performed on the flow characteristics of blood, most often the observations are made as blood or a pseudo-blood flows through rigid tubes that do not effectively represent the mechanical properties of actual blood vessels and arteries in particular.

It is well known that arteries and veins are layered vessels that have viscoelastic characteristics (Spence and Mason 1987). These vessels are comprised mostly of elastin and collagen that largely account for this viscoelastic nature. It is also generally accepted that the varying geometry of the vessel wall and the taper of the vessel have a significant effect on the flow characteristics of the vascular system (Caro *et al.* 1988). The conservation of mass requires that if there is a constricting taper present in the flow path, the average blood flow velocity will be faster at the exit than at the entrance. Previous studies have shown that the compositions of elastin, collagen, and smooth muscle present at various locations along the vessel tree directly affect the flow profiles at that particular location (Dawson 1991).

In the past researchers have endeavored to use actual blood vessels in modeling studies (Fung 1997). This is difficult since harvesting human blood vessels for study is highly regulated by the federal government. Also, blood vessels have a tendency to undergo changes in their mechanical properties upon death of the donor which leads to tainted samples. Studies of flow performed in rigid tubes have proven beneficial but do not effectively represent the effects that elasticity and vessel composition have on pressure forces and resulting velocity profile readings. Therefore, a physical model of the abdominal aorta that takes into account the viscoelasticity and varying geometry of the blood vessel would prove extremely valuable in the hemodynamic study of the major arteries in the cardiovascular system. The purpose of this study is to compare the mechanical properties of selected materials to those of canine blood vessels in order to choose which of these materials most accurately represents the viscoelasticity seen in large blood vessels.

1.2 Overview of the Human Aorta

1.2.1 Structure

The aorta is the main trunk of a series of vessels that carry oxygenated blood from the left side of the heart to the tissues of the body. It begins at the upper part of the left ventricle, where it is about 3 cm. in diameter in an average human adult, and then arches backward and to the left (Gray 1985). It then descends within the thorax on the left side of the vertebral column, passes into the abdominal cavity, and then ends by dividing into the right and left common iliac arteries. It is usually described in several portions including the ascending aorta, the arch of the aorta, and the descending aorta.

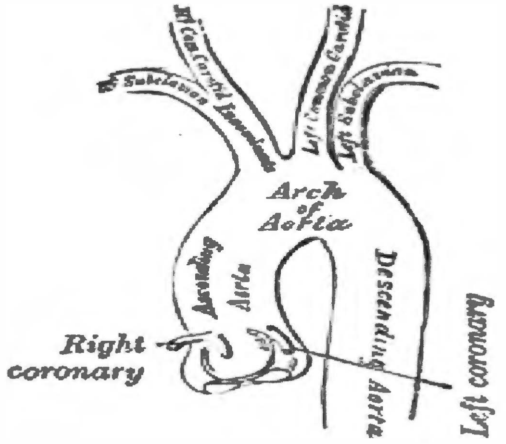

Figure 1.1: Diagram of the Aorta including the Ascending Aorta, Aortic Arch, and Thoracic Aorta (Gray 1985)

The descending aorta is composed of two portions, the thoracic and abdominal aorta (Gray 1985). The thoracic aorta is found in the posterior mediastinal cavity. It begins at the fourth thoracic vertebra and ends in front of the diaphragm. At the beginning, it is situated on the left of the vertebral column. It approaches the median line as it descends and at its termination it lies directly in front of the vertebral column. The structure of the aorta is illustrated in Figure 1.1.

The abdominal aorta begins at the lower portion of the diaphragm, in front of the lower border of the last thoracic vertebra (Gray 1985). It descends in front of the vertebral column and ends on the body of the fourth lumbar vertebra by dividing into the two common iliac arteries. It decreases in size rapidly due its large branching vessel diameters, including in particular the renal arteries.

1.2.2 Branching of the Abdominal Aorta

The branches of the abdominal aorta consist of the celiac, superior and inferior mesenteric, the left and right renal branches, and the two common iliac arteries (Bargeron *et al.* 1985). The celiac artery starts from the front of the aorta, passes nearly horizontally forward and divides into three large branches. The superior mesenteric artery begins at the front of the aorta and is crossed at its origin by the lienal vein and the neck of the pancreas. The inferior mesenteric artery starts from the aorta close to the lower border of the inferior part of the duodenum. The renal arteries start from the side of the aorta directly below the superior mesenteric artery. It lies behind the left renal vein and is crossed by the inferior mesenteric vein.

The two common iliac arteries are each about 5 cm. in length in an average human adult. They descend from the end of the aorta, passing downward and into two branches, the external iliac and hypogastric arteries which supply the lower extremity and parietes of the pelvis (Spence and Mason 1987). The right common iliac artery is somewhat longer than the left and passes more obliquely across the body of the last lumbar vertebra. The left common iliac artery lies in front of the peritoneum and the small intestines.

1.2.3 Arterial Wall Structure

Blood vessels consist of up to three relatively distinct layers: the intima, the media, and the adventitia (Jarvisalo *et al.* 2001). The intima is the innermost layer and contains endothelial cells. The middle layer is known as the media and contains a combination of collagen, elastin, and smooth muscle cells. The adventitia is the outer layer and is comprised mostly of collagen fibers and ground substances. The adventitia is considered the main source of structural stability in a blood vessel.

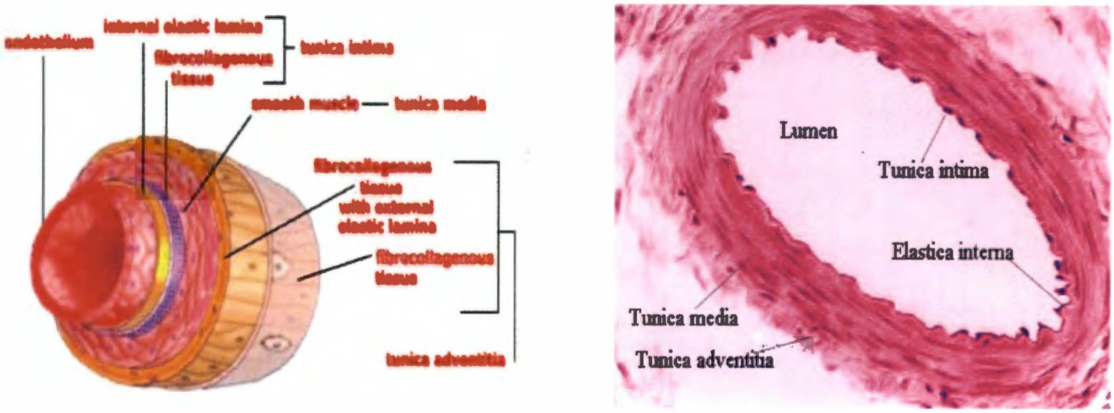

Figure 1.2: Arterial Layers (Spence and Mason 1987)

Biochemists often consider the intima synonymous with the endothelium (Levick 2003). Most anatomists define the intima as composed of the endothelial cells, the basal lamina, and the subendothelial layer composed of collagenous bundles, elastic fibrils, and smooth muscle cells. The subendothelial layer is typically present only in the larger arteries such as the aorta and its main branches. The media is made up of smooth muscle cells, a varying number of elastic sheets, bundles of collagenous fibers, and a network of elastic fibrils. The line that divides it and the adventitia is a layer of elastin. The adventitial layer is composed of collagen fibers, ground substances, and a mixture of fibroblasts, macrophages, micro blood vessels, myelinated nerves, and nonmyelinated nerves. The layers of an artery are depicted in Figure 1.2.

The structure of a large artery varies along its length (Li 2004). In large arteries, the number of lamellar layers increases with the wall thickness. In smaller arteries the wall thickness is increased, the amount of elastin is less prominent, and eventually only the inner and outer elastic lamellae can be seen as distance from the aorta increases. The variations in composition along the arterial tree are given in Table 1.1.

Table 1.1 Mass % Tissue Composition of Arterial Layers

	Pulmonary Artery	Thoracic Aorta	Plantar Artery
Media			
Smooth Muscle	46.4	33.5	60.5
Ground Substance	17.2	5.6	26.4
Elastin	9.1	24.3	1.3
Collagen	27.4	36.8	11.9
Adventitia			
Collagen	63	77.7	63.9
Ground Substance	25.1	10.6	24.7
Fibroblasts	10.4	9.4	11.4
Elastin	1.5	2.4	0

1.3 Mechanical Behavior of Arterial Tissue

1.3.1 Behavior under Uniaxial Loading

Stresses and strains vary across the thickness of an arterial wall making the modeling of these properties a three dimensional problem. Assuming that the vessel is a thin-layered material, these stresses and strains can be separated into two parts; the mean values and the deviations from the means. The mean circumferential, longitudinal and shear stresses are all considered uniform across the wall. The principles governing these mean stresses are reflected in the same equations as those governing a shell whose wall thickness is very small. Therefore, if only the mean values are of interest, then the three dimensional problem can be reduced to a two dimensional one. In this case, the constitutive equation used is the one relating membrane stress with the membrane strain in two orthogonal directions.

In the case of the arterial wall being considered as a thin membrane, the simplest experiment for evaluating the mechanical properties of a blood vessel that can be done is a uniaxial test (Fung 1997). This involves taking a longitudinal or circumferential strip of vessel wall tissue and pulling it lengthwise while recording the force-elongation relationship. The tensile stress T can be represented by:

$$T = \frac{load}{A_o} = f(\lambda)$$

where A_O is the cross-sectional area of the specimen and T is a function of the length to initial length ratio λ. Studies on arterial wall tissue performed by Fung (1997) have shown that after a sufficient number of tests the stress-strain loop is stabilized and does not change further. The stress can then be related to the strain in the form:

$$T = f_1(\lambda) \text{ when } \frac{d\lambda}{dt} > 0$$

$$T = f_2(\lambda) \text{ when } \frac{d\lambda}{dt} < 0$$

where f_1 and f_2 are two independent functions. If $f_1(\lambda) = f_2(\lambda)$, then the material is purely elastic in character. If the functions are not equal then the material can be either inelastic or possibly viscoelastic.

One way to examine the functions $f_1(\lambda)$ and $f_2(\lambda)$ is to plot the slope of $d\lambda/dt$ versus T (Dobrin 1978). If an arterial tissue section obeys Hooke's law, then the experimental data plot will show a horizontal straight line. For a tensile stress greater than 20 kPa but less than 60 kPa, which would be representative of a physiological range (Wuyts *et al.* 1995), the following approximation was derived from the data plot:

$$\frac{d\lambda}{dt} = \alpha(T + \beta) = \alpha T + E_o$$

where α, β, and E_O are constants. This equation implies an exponential stress-strain relationship of the form:

$$T = \left(T^{*} + \beta\right)e^{\alpha\left(\lambda + \lambda^{*}\right)} + \beta \text{ for } 20 < T < 60 \text{ kPa.}$$

Where T* and λ* are time averaged properties for tensile stress and Lames' constant, respectively.

The parameter α represents the rate of increase of the Young's modulus with respect to the time elapsed (Hensley 2001). The parameter E_O is the intercept of the straight-line segment extended to T = 0. E_O has been found to vary significantly along the length of the aorta and its values for longitudinal segments can vary from those of the circumferential segments (Kuecherer *et al.* 2000). These differences reflect the changes in material composition and configuration of collagen, elastin, and smooth muscle fibers in the arterial wall along the length of the aorta.

1.3.2 Collagen Properties

Collagen is the basic structural component for hard and soft tissues in humans. It is responsible for the strength and mechanical integrity of our bodies (Fung 1997). Studies of collagen fibers present in skin, arteries, and tendons indicate that the elastic modulus is in the range of 0.3 to 2.5 MPa depending on the amount of extension (Monson 2001). The heightened stiffness that results from increased extension is associated with the increasingly parallel alignment of the fibers. "Pure" collagen fibers can only be extended to relative strains of 0.03 to 0.04 before breaking. This is much smaller than the amount of strain to which arteries can be extended which suggests that collagen in arteries must be relatively unstretched until the artery is highly extended. At large strains both collagen fibers and intact arteries have been shown to become somewhat inextensible.

1.3.3 Elastin Properties

Elastin is one of the most "linearly" elastic biosolid materials known. Load extension data indicate that elastin is extremely extendable (Fung 1995). It behaves mechanically as though it were composed of long independent chains. Several studies have shown the elastic modulus of elastin to be in the range of 1.5 to 4.1 MPa (Schulze-Bauer and Holzapfel 2002). In general, the modulus tends to increase in a curvilinear manner with extension. It has been shown that elastin fibers extend to relative strains up to 1.3 to 1.6 before breaking occurs. Such a large strain is evidence that the extensibility of elastin fibers is a result of not only the properties of these fibers but also their network alignment (Schulze-Bauer and Holzapfel 2002).

1.3.4 Arterial Tissue Mechanical Properties

One of the most defining mechanical characteristics of arterial tissue is that it becomes stiffer when stretched (Wuyts *et al.* 1995). This corresponds to the large number of collagen fibers in the adventitial layer. This finding has been reported for length-force studies of strips of arteries as well as in-vitro pressure–volume studies of intact arteries (Wuyts *et al.* 1995). The comprehensive result of these pressure-volume studies was the derivation of the "pressure elastic modulus" which is a property that closely resembles the elastic modulus and can be readily applied to arteries in-vivo. The pressure elastic modulus, E_v, is represented by:

$$E_v = \frac{\Delta P \times r}{\Delta r}$$

where ΔP is the change in pressure across the vessel wall, and Δr is the variation in radius during each cardiac cycle.

E_v calculated for the human abdominal aorta was found to range from 0.16 to 0.36 MPa (Zulliger *et al.* 2004). It was found that for all vessels, E_v tends to rise with increasing pressure as well as with distance from the heart. This corresponds to the distribution of tensile strength of arteries as well as the distribution of collagen along the arterial tree.

Extension has been associated with increased stiffness in arteries (Silver *et al.* 2003). It has been implied by many researchers that this property reflects the extensibility of elastin at small strains and the stiffness of collagen at high strains. There is also evidence that elastin bears the majority of the circumferential load at small extensions and that collagen bears the longitudinal and circumferential loads at physiological and higher extensions (Silver *et al.* 2003).

The variation in composition as well as the alignment of collagen and elastin in the arterial wall is responsible for the biaxial elastic properties of the vessels (Lee and Yen 2002). Elastin, which is found mainly in the elastic lamellae of the media, lies parallel to the long axis of the vessel and is concentric to the vessel lumen. This alignment allows elastin to bear both longitudinal and circumferential loads at low strains. The large concentration of collagen in the adventitial layer has been found to predominantly bear longitudinal loads at higher strains. This is due to the fact that there tends to be no systematic alignment of these fibers in the adventitia. This random alignment results in a balance in the resistance to longitudinal and circumferential loading.

1.3.5 Mathematical Representation of the Stress-Strain Relationship

In the past the stress-strain relationship in blood vessels has been described mathematically. This has proven useful when designing computational blood vessel models based on experimental data. There are many forms of the mathematical equations which have been used to describe the stress-strain relationship. In the case of mechanical testing there are basically only two schools: one uses polynomials, the other uses exponential functions to describe nonlinear effects (Fung 1997). In a two-dimensional case the strain-energy function $\rho_o W$ (ρ_o = tissue density, W = energy function) is a function of $E_{\theta\theta}$ and E_{zz} if shear isn't involved. Most researchers prefer to use the exponential form of the equation defined as:

$$\rho_o W = \frac{C}{2} \times \exp\left[a_1\left(E^2{}_{\theta\theta} - E^*{}_{\theta\theta}{}^2\right) + a_2\left(E^2{}_{zz} - E^*{}_{zz}{}^2\right) + 2a_4\left(E_{\theta\theta}E_{zz} - E^*{}_{\theta\theta}E^*{}_{zz}\right)\right]$$

where $\rho_o W$ is the strain energy function, C and a_1, a_2, a_4 are material constants and $E^*_{\theta\theta}$ and E^*_{zz} are strains corresponding to an arbitrarily selected pair of stresses $S^*_{\theta\theta}$ and S^*_{zz} (Fung 1995). The asterisk quantities can be absorbed into the constant C to yield the form:

$$\rho_o W = \frac{C}{2} \times \exp\left[a_1\left(E^2{}_{\theta\theta}\right) + a_2\left(E^2{}_{zz}\right) + 2a_4\left(E_{\theta\theta}E_{zz}\right)\right]$$

The utility of these mathematical representations can be demonstrated in two ways. First, the ability of the function to fit actual experimental data over a full range of strains of interest can be evaluated. Second, the usefulness of the parameters in distinguishing the members of a family of stress-strain curves can be evaluated. For the exponential strain-energy function, the constants C, a_1, a_2, a_4 can be determined by minimizing the sum of the squares of the differences between the experimental and theoretical data.

The overall fit for the exponential function is considered to be sufficient since little deviation from the mean values of stress and strain data is seen after repeated testing. The standard deviations of the material constants a_1, a_2, and a_4 for large arteries have a tendency to be very large for some data sets (Schvartzman *et al.* 2002). Also, some of the coefficients have been found to change signs in different runs of the same experiment. These changes are caused by the sensitivity of the coefficients to relatively small changes in the shape of the stress-strain curves. The overall smaller variation in the coefficients is the main reason why the exponential data correlation is preferred by most researchers.

1.4 Summary of Previous Studies

Segers *et al.* (1998) studied simulated pulsatile flow in the human aorta by extending an existing human pulse duplicator system with an elastic tube model of the arterial tree to produce a cardiovascular simulator. The model was made of natural latex rubber and included sections that simulated the aorta, the upper and lower limb arteries, the carotid arteries and the major aortic branches to the abdominal organs. Pressure was measured at six locations along the aorta, together with the aortic flow. The study demonstrated a correspondence between the high frequency phase velocity components and the axial velocity along the entire model. The model also demonstrated reflections at the level of the renal and sphlenic arteries. It was concluded from this study that a substantial similarity between the in vivo observations and the model results existed and therefore the model was an effective tool for the study of pulsatile flow in elastic vessels.

Fung *et al.* (1993) presented a method of determining the mechanical properties of the different layers of porcine blood vessels in vivo. With this proposed method, vessels with a diameter of 100 μm and up could be observed and mechanical properties could be obtained for the vascular smooth and adventitia components. In order to obtain the desired data, the researchers first determined the zero stress state. They then obtained metamorphic data on the thickness of each layer and made mechanical measurements in the neighborhood of the zero stress state. Eight small perturbation experiments were done on each blood vessel to determine the elastic moduli of the two layers of the blood vessel wall. Under the assumption that the intima-media layer represented 50% of the total thickness, the study found that the elastic moduli were 447.5 kPa for the intima-media layer and 111.9 kPa for the adventitial layer.

Silver *et al.* (2003) utilized previously developed incremental stress-strain curves to study the mechanical behavior of the porcine aorta, carotid artery, and the vena cava in vivo. The study focused on the high and low strain portions of the curves that were found to be approximately linear. Analysis at low strains showed that the behavior is dominated by the elastic fibers, and that the elastic and collagen fibers were in parallel networks. The study also showed that the high strain behavior differed from the behavior of skin, which is dominated by collagen fibers. The high strain behavior was found to be consistent with the series arrangement of the collagen and smooth fibers in blood vessels. It was also concluded that the mechanical behavior of the vessel wall differs from the behavior of other extracellular matrices that do not contain smooth muscle. The main conclusion drawn from this study was that the arrangement of the collagen and smooth muscle was a significant factor in determining the mechanical behavior of the vessels and these arrangements vary among different vessels.

Bauer *et al.* (2002) studied the mechanics of the human femoral adventitia on the basis of adventitial tube tests utilizing a thin-walled model. Inflation tests of 11 nonstenotic arteries were performed after autopsy. Adventitial tubes underwent cyclic, quasistatic extension-inflation tests using high pressures up to 100 kPa. The study showed that at physiological blood pressure (13.3 kPa), the adventitia carries approximately 25% of the pressure load in the vessel wall, whereas their circumferential and axial stresses were similar to the total wall stresses supporting a "uniform stress hypothesis". This study also found that at higher pressures the adventitia becomes the mechanically predominant layer, carrying greater than 50% of the load. Based on these findings, the mechanical role of the adventitia at physiological and hypertensive states was characterized.

Wuyts *et al.* (1995) developed a model for the tension-radius relationship of blood vessels that took into account the mechanical constituents collagen, elastin, and smooth muscle. The model incorporated four characteristic parameters: the Young's modulus of the collagen fibers, the Young's modulus of the combined smooth muscle/elastin network, the amount of strain at which the high stiffness region of the tension-radius curve is reached, and an indicator for the degree of collagen fiber stretching. This model made possible an objective comparison of the mechanical properties of various blood vessel types based on the mechanically predominant parameters previously mentioned. The model was successfully fitted to the tension-radius data of 65 human aortas with moderate or severe atherosclerosis. The study demonstrated that the structural and global stiffness changes associated with age increases approximately ninefold over 60 years.

Poutanen *et al.* (2003) studied the normal aortic dimensions and flow in 168 children and young adults. The purpose of the study was to determine normal values for aortic dimensions with two-dimensional echocardiography and for aortic flow velocities with Doppler echocardiography in healthy children and young adults. The dimensions and flow were obtained at the aortic annulus, aortic sinus, sinotubular junction, at the origin of the innominate artery, at the origin of the carotid artery, at the subclavian artery, and on the descending aorta near the diaphragm. The study found that all vessel diameters correlated closely with age, body surface area, height, and weight. The diameters of the ascending and descending aorta were found to be similar in both genders when indexed to body surface area.

Chapter 2

Materials and Methods

2.1 Candidate Materials for Arterial Model Study

A blood vessel can be described as a nonhomogenous, viscoelastic material (Summers *et al.* 1998). These characteristics are difficult to simulate with a single isotropic material since most manufacturing processes are limited to producing a material with a homogenous composition. This most often results in the same mechanical properties throughout the material. This study focused on comparing selected candidate materials that show both elastic and plastic characteristics. Once a suitable material is identified, it can then be modified to more effectively represent the mechanical properties of a blood vessel.

The candidate materials used for testing were selected among commercially available soft plastics and elastomers. These materials were obtained from McMaster-Carr Supply Company (Atlanta, Georgia). The candidate materials were selected in a manner that represented a wide range of mechanical properties. This maximized the likelihood that the properties of blood vessels could be effectively modeled with the choice of an appropriate material. Although extensive data on the mechanical properties of these materials exist it was important to conduct specific uniaxial tensile tests on the selected materials in order to ensure continuity between the results of this testing and that of the vascular tissue studied. Typical reported values for the yield strength and elastic modulus of these selected materials is given in Table 2.1.

Table 2.1 Mechanical Properties of Candidate Materials

	ESPU	ETPU	LDPE	PP	Ny.11	EVA	PE-EVA	San	Vit	Neo	Sil. Rub
Yield Strength (Mpa)	9 to 13	5 to 12	8 to 15	30 to 36	62 to 68	8 to 10	13 to 18	5 to 10	0.5 to 3	1 to 4	1 to 5
Elastic Modulus (Mpa)	1 to 5	2 to 7	9.5 to 12	125 to 140	135 to 145	120 to 150	150 to 180	0.5 to 3	0.1 to 1	0.4 to2	0.1 to 2

2.1.1 Plastics

The two types of polyurethanes used in this study are part of a class of urethanes called thermoplastics. They are linear block copolymers that are synthesized from general types of urethane components, namely a diisocyanate, a polyol and a chain extender (Feldman and Barbalata 1996). The main difference between the two is that the ether-based urethanes (ETPU) are stronger and stiffer and the ester-based urethanes (ESPU) are more flexible.

Polyethylenes are olefin polymers that are the most commonly manufactured thermoplastic material (Feldman and Barbalata 1996). There are several well-established families of polyethylenes. The most common of these families are low-density polyethylene (LDPE) which was used in this study. Polyethylenes are long chains of the ethylene molecule that are produced from petroleum and natural gas.

Polypropylene (PP) is a major thermoplastic material that ranks only behind polyethylene and PVC as far as production demands are concerned (Feldman and Barbalata 1996). Polypropylenes are chains of molecules composed of hydrogen, carbon, and a methyl group. There are three main categories of polypropylenes produced commercially: homopolymers, copolymers and blends.

Nylon 11 is from a family of materials that are comprised of different compositions of linear aliphatic polyamides (Feldman and Barbalata 1996). The difference between the types of nylons, all designated by a specific number, is the number of monomers found in the molecular chains. Nylon 11 is known for its relatively high yield strength and elastic modulus.

Ethylene vinyl acetate (EVA) is a random copolymer where the content of vinyl acetate varies between 5 and 50% (Feldman and Barbalata 1996). This varied content of vinyl acetate is what controls the crystallinity and the flexibility of the materials. Depending on the composition and molecular weight of the EVA copolymer, they have a low softening point and are often used as wax additives.

Polyethylene-lined EVA (PE-EVA) is a variation of the EVA copolymer where polyethylene is added to increase the mechanical integrity of the material (Feldman and Barbalata 1996). A polyethylene liner and an EVA outer shell combine for a material that resists freezing and withstands fluctuating temperatures while remaining flexible and impact resistant. Polyethylene-lined EVA has a higher resistance to abrasion and a higher tensile strength

2.1.2 Elastomers

Santoprene is a combination of EPDM rubber and polypropylene plastic (Feldman and Barbalata 1996). It is known for being highly durable, resistant to fatigue and cracking, and resistant to ozone and ultraviolet light at high temperatures. Santoprene is more durable than natural rubber, and its more resilient, flexible, and softer then most plastics.

Neoprene is an extremely versatile synthetic rubber with a basic chemical composition that consists of polychloroprene (Feldman and Barbalata 1996). It was originally developed as an oil-resistant substitute for natural rubber. Neoprene is noted for its resistance to degradation, resistance to flexure and torque, and its ability to resist chemical decomposition when it comes into contact with corrosive agents.

Viton is the most specified of the fluoroelastomers. It is well known for its excellent abrasion resistance (Feldman and Barbalata 1996). Viton consists of four types of families: A, B, F, and Extreme-TBR. The four families differ primarily in polymeric structure as well as in composition.

Silicone rubbers are a class of rubbers that incorporate linear macromolecules which increase the molecular weight of the material (Feldman and Barbalata 1996). Silicone rubbers are known for having good wear resistance and high flexibility. They are also known to be resilient after experiencing relatively high loads.

2.1.3 Canine Blood Vessels

The canine aortic vessels used in the longitudinal and circumferential testing in this study were obtained from Dr. Joseph Weigel, Professor of Small Animal Clinical Sciences at the University Of Tennessee College Of Veterinary Medicine. Five specimens with a length of approximately 12 cm and diameter of 1.5 cm were dissected from young adult canine species in good health between 3-5 years of age. The canines were mostly large mixed breeds with one being a pure bred Rottweiler. The specimens were thoracic aortas taken from the aortic arch to the region of the diaphragm. The canines were euthanized due to various injuries; no diseases were present in any of the donors.

The longitudinal specimens were placed in a saline-electrolytic solution and refrigerated at approximately 40^{0}F for up to one month while specimen preparation and testing were completed. The circumferential specimens were also placed in a saline-electrolytic solution and stored for approximately three days before testing was conducted. In both cases, the specimens were prepared immediately after they were obtained from Dr. Weigel. They were then subjected to their various storage periods until testing occurred. In order to assure continuity of test results between the plastics as well as the vessels, the canine test specimens were cut to the appropriate lengths and widths according to ASTM standard D 882.

2.2 Experimental Methods

2.2.1 Apparatus

Uniaxial tensile testing of the canine aorta specimens and the candidate materials was performed on a 450 N Capacity Instron, Model 1122 Tensile Testing Machine. The machine was located at the University of Tennessee Textiles and Nonwovens Development Center (TANDEC) facility on the Knoxville campus. This particular model was designed for testing small specimens, thin sheet, or wire. It can also be set up for compression testing and for transverse rupture strength of cemented carbides. The machine was equipped with a 72W x 75D x 100L cm, 450 N load frame testing console. The available testing speed ranges from 0.055 to 125 cm/s. The Instron machine used in testing is pictured in Figure 2.1

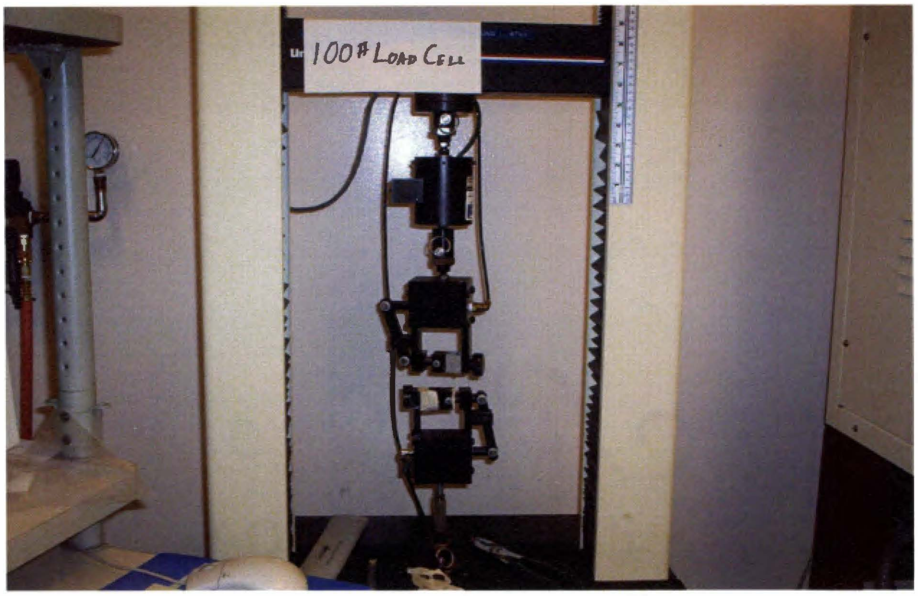

Figure 2.1: Instron 1122 Model Tensile Tester

2.2.2 Candidate Material Preparation

Candidate materials were cut to the appropriate lengths and widths outlined in ASTM standard 882. This standard requires that the length to width ratio be at least 5:1. The candidate materials were obtained in tubing form in order to obtain the desired thicknesses. Three specimens were prepared for each candidate material. The materials were cut through the midline using a pair of surgical scissors. The materials were then cut to the desired dimensions. The lengths were cut as close to 8.0 centimeters as possible. The widths were cut to as close to 0.50 cm as was possible. The dimensions were measured using a Vernier caliper. The lengths, widths, and thicknesses were measured at four different places along the test specimen and the means and standard deviation were then calculated. A length to width ratio value of approximately 16:1 was reported for each material. The lengths, widths, and thicknesses of the candidate material samples along with their standard deviations are given in Table 2.2.

Table 2.2: Candidate Material Test Specimen Dimensions

Material	L (cm)	STD. DEV. (cm)	W (cm)	STD. DEV. (cm)	Thickness (cm)	STD. DEV. (cm)
Ester PU	8.04	0.019	0.525	0.48	0.16	0.006
Ether PU	8.145	0.016	0.52	0.016	0.161	0.007
LDPE	8.05	0.028	0.525	0.019	0.154	0.005
PP	8.1	0.049	0.55	0.048	0.147	0.002
Nylon 11	8.06	0.066	0.56	0.029	0.156	0.004
EVA	7.97	0.023	0.515	0.036	0.151	0.001
PE-EVA	7.95	0.045	0.535	0.038	0.159	0.008
Santoprene	8.01	0.014	0.52	0.028	0.158	0.008
Viton	8.14	0.045	0.53	0.045	0.159	0.006
Neoprene	8.05	0.038	0.545	0.038	0.153	0.009
Silicone	7.96	0.045	0.538	0.045	0.158	0.003

The values in Table 2.2 show that the dimensions for each candidate material vary to a small degree. The variations shown in these dimensions are due to the lack of precise sample sizing instruments and human error. The goal when preparing the specimens was to achieve dimensions that were equal for the various samples tested. Despite the variations indicated it was concluded that these small differences did not cause any major changes in the values reflected in the data plots. Since stress is defined as force divided by area, minor to modest variations in the dimensions will be accounted for in this calculation.

2.2.3 Vessel Preparation

The blood vessels for longitudinal and circumferential testing were cut to the appropriate lengths and widths that are outlined in ASTM standard 882 Three specimens were prepared for each blood vessel utilized in longitudinal testing. As with the candidate materials, the blood vessels were cut through the midline using a pair of surgical scissors.

Table 2.3: Blood Vessel Test Specimen Dimensions

Material	L (cm)	STD. DEV.	W (cm)	STD. DEV.	t (cm)	STD. DEV.
Longitudinal-day	7.76	0.054	0.515	0.054	0.144	0.002
Longitudinal-week	7.96	0.064	0.53	0.046	0.154	0.005
Longitudinal-month	7.88	0.035	0.505	0.028	0.154	0.005
Circumferential	3.42	0.025	0.248	0.055	0.161	0.004

The blood vessels were then cut to the desired dimensions. The lengths were cut as close to 8.0 centimeters as possible. The widths were cut to as close to 0.50 cm as was possible. The dimensions were measured using a Vernier caliper. The lengths, widths, and thicknesses were measured at four different places along the test specimen and the means and standard deviation were then calculated. A length to width ratio value of approximately 16:1 was reported for each test specimen. This ratio was desirable since it would ensure that a uniform stress is placed in the gauge length of the specimen. This ratio also helps to ensure that the specimen will break within the gauge length. The lengths, widths, and thicknesses of the blood vessel samples along with their standard deviations are given in Table 2.3.

When preparing the circumferential sample the dimensional requirements had to be altered since the length of these specimens was limited by the circumference of the vessel itself. The maximum length of the circumferential samples was limited to πD where D is the diameter of the vessel. This yielded a maximum length of approximately 3.5 cm. The width of the specimens were cut as close to 0.5 cm as possible. This gave a length to width ratio value of approximately 7:1. In retrospect, the potential candidate material samples could have been sized to correspond to the limited vessel dimensions

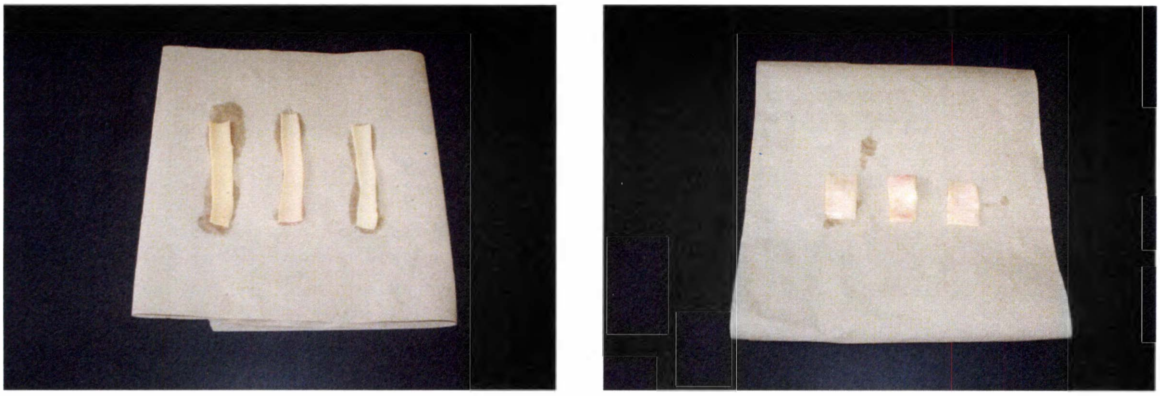

A) Longitudinal B) Circumferential

Figure 2.2: Vessels Prepared for Testing

but the comparative data was deemed suitable. ASTM criteria were met for all candidate materials and vascular tissue samples tested.

As with the candidate materials, the values in Table 2.3 show that the dimensions for each vessel vary to a small degree. The variations shown in these dimensions are due to the lack of precise sizing instruments, the inconsistent composition among the vessels tested, and human error. Despite the variations, these differences were small and were judged to not cause any major changes in the values obtained from the data plots. The variations in these dimensions are therefore neglected in this part of the study. The appearance of the tested specimens is depicted in the photographs in Figure 2.2.

2.2.4 Testing Procedure

Due to equipment limitations, experimental testing of both the candidate materials and the arterial tissue was limited to uniaxial tensile tests. These tests were performed according to ASTM 882. ASTM standard 882 requires testing rectangular strips to ensure that a uniform stress is placed on all tested specimens. This in turn allows the crosshead displacement to be directly related to the specimen strain. This ASTM standard calls for a population of at least three specimens in each sample being tested.

The dimensions of the tested specimens are reported in Section 2.2.2 and.2.2.3. The lengths and widths were measured to an accuracy of approximately 0.25 mm and the thicknesses were measured to an accuracy of approximately 0.003 mm. The initial grip separation (gauge length) was set to 2.54 cm for testing in the longitudinal direction and 0.75 cm for testing in the circumferential direction to account for the shorter length of these strips. The rate of grip separation was set to 500 mm/min. in all cases. This is in compliance with the testing rates given in Figure 2.3.

Once these steps were, completed testing began by placing the specimen in the grips of the testing machine. The specimens were all placed carefully so that the long axis was aligned with an assumed line joining the points of attachment of the grips to the machine. The canine specimens remained in a saline solution until a few minutes before testing to ensure that they remained moist during the procedure. The specimens were then stretched until breaking occurred or the 450 N maximum load was achieved. The raw data from testing were exported to an Excel file in a Dell 2400 PC where the force and extension data were converted to stress and strain values from which the desired data plots were constructed utilizing the Excel program.

Percent Elongation at Break	Initial Strain Rate, mm/mm·min (in./in.·min)	Initial Grip Separation		Rate of Grip Separation	
		mm	in.	mm/min	in./min
		Modulus of Elasticity Determination			
	0.1	250	10	25	1.0
		Determinations other than Elastic Modulus			
Less than 20	0.1	125	5	12.5	0.5
20 to 100	0.5	100	4	50	2.0
Greater than 100	10.0	50	2	500	20.0

Figure 2.3: Standard Testing Rates Specified in ASTM Standard 882

2.2.5 Statistical Analysis

In order to analyze the collected data a student t-test for independent samples was utilized. Utilizing this method of statistical analysis ensures that an effective comparison of the populations tested is achieved. The goal was to compare the circumferential and longitudinal values for yield strength, elongation at yield, elongation at break, maximum stress, maximum strain, and elastic modulus to the same mechanical properties of the polymer samples. It was also important to determine if the same properties of the vessels varied with the longitudinal or circumferential direction of testing. The effects of storing the vessels for a period of one week and one month were also examined using this method.

The student t-tests utilized in the time dependency analysis, the directional dependency analysis, and the polymer/blood vessel comparisons all followed the same format. The null hypothesis, H_o, was that the mean property values for both samples being compared were equal: $\mu_1 = \mu_2$. The alternative hypothesis, H_1, was that the mean property values of the two samples being compared were not equal: $\mu_1 \neq \mu_2$. The test statistic, t, had the following form:

$$t = \frac{X_1 - X_2}{\sqrt{\frac{s_n^{\,2}}{n} + \frac{s_m^{\,2}}{m}}}$$

where X_1 is the mean value of he property being compared for the day-old blood vessels, X_2 is the mean of the same property for the samples being compared, s_n^2 is the variance of the day-old blood vessels, s_m^2 is the variance of the samples being compared and n and m are the sample populations (n = m = 3).

Once the test statistic was calculated, statistical significance was determined utilizing the table of the t-distribution (Degroot 2002). Since this study has a sample population of three for each candidate material and blood vessel, a degree of freedom value of two is taken for the statistical analysis. Statistical significance was assumed at $p \leq 0.05$. This gave a critical value of 9.925 from the table of the t-distribution. If the calculated test statistic was less than this value, the null hypothesis that the sample means are equal was accepted and the material or vessel was given a grade of pass for the specific property being compared. Otherwise, the alternative hypothesis was accepted and the material or vessel was given a grade of fail for the specific property being compared. Correlations between the data sets were considered significant at the 0.01 level (2-tailed).

Chapter 3

Results and Discussion

3.1 Overview of Results

The results of the uniaxial tensile testing performed on the canine aortic tissue specimens and candidate materials are reported together in Table 3.1. The values for the imposed stress and resulting strain for each material are plotted and discussed in Section 3.2. The yield strength and elongation at yield values are obtained from the point on each individual data plot where the slope of the stress-strain curve approaches zero after an initial high slope. Elongation at break was found at the end of the curve at the point where the candidate material or vessel breaks. Stress and strain maximums were obtained by utilizing the MAX(Z) command in the EXCEL program which gives the maximum value over a specified data range, Z . Elastic modulus values were determined by a calculation of the slope of the elastic region of the stress-strain curve.

The experimental runs were conducted initially by trial and error with slippage often occurring at the material-grip interface. After placing sand paper on the grips and making a few practice runs, the tests began to go much more smoothly with no discernable slipping. The results of the experiments performed are reported and discussed in the following sections of this chapter.

3.1.1 Time Dependency of Experimental Data

The statistical analysis described in Section 2.2.5 was utilized to determine whether or not the properties of the canine specimens prepared for longitudinal testing vary significantly over specific periods of storage.

Table 3.1: Mechanical Properties Derived from Experimental Data

Model Materials	Yield Strength (MPa)	Elongation at Yield (cm)	Elongation at Max (cm)	Stress Max (MPa)	Strain Max	Elastic Modulus (MPa)
Soft Ester PU	0.2083	0.7057	0.6611	1.507	18.1	0.298
Ether PU	0.4948	0.994	0.2993	2.49	11.78	0.587
LDPE	0.387	0.5936	0.4534	0.664	17.85	1.01
PP	0.4486	0.046	0.0246	0.459	0.966	11.17
Nylon 11	0.551	0.112	0.038	0.922	1.51	5.08
EVA	0.226	0.736	0.222	0.389	8.75	0.469
PE-EVA	0.206	0.387	0.369	0.525	14.56	0.635
Santoprene	0.082	0.265	0.169	0.247	6.65	0.341
Viton	0.03	0.099	0.166	0.293	2.61	0.314
Neoprene	0.043	0.138	0.162	0.311	2.45	0.315
Silicone Rubber	0.115	0.471	0.516	0.234	3.56	0.217
Longitudinal-Day	0.135	0.57	0.582	0.135	2.245	0.225
Longitudinal-Week	0.135	0.56	0.57	0.134	2.244	0.2139
Longitudinal-Month	0.134	0.556	0.57	0.135	2.25	0.212
Circumferential	0.1347	0.562	0.574	0.1558	2.262	0.248

This study focused on the yield strength, elongation at yield, elongation at break, maximum stress, maximum strain, and the elastic modulus of those vessels tested. The results from one week and one month were compared to the results from one day since it is best to test biological soft tissues as soon as possible after extraction has occurred. The results were considered significant at the 0.01 level. In other words, if the one week or one month sample being compared to the one day sample passed the t-test for a specific mechanical property then there was a 99% probability that the vessel was similar to the day-old sample for that specific value.

In the case of the one week longitudinal strips, yield stress values did not vary from the one day sample ($p \leq 0.01$). The elongation at yield was determined to be statistically similar to the one day sample ($p \leq 0.01$). The elongation at break was found to vary slightly more than the elongation at yield but was likewise determined to be statistically similar ($p \leq 0.01$). The maximum stress and strain values observed in the week-old sample did not vary from the one day sample ($p \leq 0.01$). The elastic modulus was statistically similar to the one day sample ($p \leq 0.01$).

In the case of the one month longitudinal strips, yield stress values did not vary from the one day sample ($p \leq 0.01$). The elongation at yield was determined to be statistically similar to the one day sample ($p \leq 0.01$). As with the one week sample, the elongation at break was found to vary slightly more than the elongation at yield but was likewise determined to be statistically similar ($p \leq 0.01$). The maximum stress and strain values observed in the month-old sample were determined to be statistically similar to the one day sample ($p \leq 0.01$). The elastic modulus values did not vary from the one day sample ($p \leq 0.01$). The results of the statistical analysis for all values are presented in Table 3.2.

When comparing the day-old property values to the week-old values it was found that there was a 0.295% difference between the yield strength, a 0.045% difference between the maximum strain, and a 4.5% difference between the elastic modulus. When comparing the day-old values to the month-old values it was found that there was a 0.745% difference between the yield strength, a 0.22% difference between the maximum strain values, and a 5.5% difference between the elastic modulus.

3.1.2 Directional Dependency of Experimental Data

The statistical analysis described in Section 2.2.5 was utilized to determine whether or not the properties of the canine specimens vary for tissue samples cut longitudinally or circumferentially. Again, this study focused on the yield strength,

Table 3.2: Results of Statistical t-Test for Longitudinal Values ($p \leq 0.01$)

Material	Yield Strength (MPa)	Elongation at Yield (cm)	Elongation at Break (cm)	Stress Max (MPa)	Strain Max	Elastic Modulus (MPa)
Ester PU	fail	fail	fail	fail	fail	pass
Ether PU	fail	pass	fail	fail	fail	pass
PE	fail	pass	fail	fail	fail	fail
PP	fail	pass	fail	fail	fail	fail
Nylon 11	pass	pass	fail	fail	fail	fail
EVA	fail	fail	fail	fail	pass	pass
PE-EVA	fail	fail	fail	fail	fail	pass
Santoprene	fail	fail	fail	pass	fail	pass
Viton	fail	pass	pass	pass	pass	pass
Neoprene	pass	fail	pass	fail	pass	pass
Silicone	pass	pass	pass	pass	pass	pass
Longitudinal-week	pass	pass	pass	pass	pass	pass
Longitudinal-month	pass	pass	pass	pass	pass	pass
Circumferential	pass	pass	pass	pass	pass	pass

elongation at yield, elongation at break, maximum stress, maximum strain, and the elastic modulus of those vessels tested. The results were considered significant at the 0.01 level.

In the case of the circumferential specimens, the yield strength values were found to be similar to the results for the one day, one week, and one month longitudinal sample ($p \leq 0.01$). The elongation at yield was found to be similar to the day one day, one week, and one month longitudinal sample longitudinal sample ($p \leq 0.01$). The elongation at break was found to be similar to the one day, one week, and one month longitudinal sample ($p \leq 0.01$). The maximum stress and strain values were determined to be statistically similar to the one day, one week, and one month longitudinal sample ($p \leq 0.01$). The elastic modulus values were found to be similar to the one day, one week, and one month longitudinal sample longitudinal sample ($p \leq 0.01$). The results of the statistical analysis for all values are presented in Table 3.2.

The circumferential tissue specimens were tested after being stored for a period of approximately 72 hours due to the lack of availability of the testing facilities during the weekend. Therefore the specimens were compared to the day-old longitudinal samples for percent differences. The yield strength values were found to have a 0.25% difference. The elongation at yield was found to have a 1.40% difference. The elongation at break was found to have a 1.37% difference. The maximum stress values were found to have a 10.9% difference. The maximum strain values were found to have a .75% difference. The elastic modulus values were found to have a 5.46% difference.

3.1.3 Candidate Material /Blood Vessel Comparison (Longitudinal)

The statistical analysis described in Section 2.2.5 was utilized to determine which candidate material is most similar in mechanical behavior to the blood vessel tissue samples being studied. This study focused on the same mechanical properties involved in the previous comparisons. The goal was to determine if any of the materials are similar to all of the mechanical properties of the blood vessels. The results were considered significant at the 0.01 level.

For the yield strength values, nylon 11, santoprene, and viton were all found to vary from the one day longitudinal strips ($p \leq 0.01$). Ester-based polyurethane, ether-based polyurethane, polyethylene, polypropylene, EVA, polyethylene-lined EVA, neoprene and silicone rubber were all found to have yield strength values statistically similar to the one day longitudinal strips ($p \leq 0.01$).

The elongation at yield was found to vary with the ether-based polyurethane results ($p \leq 0.01$). Ester-based polyurethane, ether-based polyurethane, polyethylene, polypropylene, EVA, polyethylene-lined EVA, santoprene, viton, neoprene, and silicone rubber were all found to have an elongation at yield that were statistically similar to the one day longitudinal strips ($p \leq 0.01$).

The elongation at break was found to be statistically similar for viton, neoprene, and silicone rubber ($p \leq 0.01$). Ester-based polyurethane, ether-based polyurethane, polyethylene, polypropylene, nylon 11, EVA, polyethylene-lined EVA and santoprene were all found to have an elongation at break that varied from the one day longitudinal strips ($p \leq 0.01$).

For the maximum strain values, EVA, santoprene, viton, neoprene, and silicone rubber were found to be statistically similar to the one day longitudinal strips ($p \leq 0.01$). Ester-based polyurethane, ether-based polyurethane, polyethylene, polypropylene, nylon 11, and polyethylene-lined EVA were all found to have maximum stress values that varied from one day longitudinal strips ($p \leq 0.01$).

For the maximum strain values EVA, viton, neoprene, and silicone rubber were all found to have values that were statistically similar to the one day longitudinal strips ($p \leq 0.01$). Ester-based polyurethane, ether-based polyurethane, polyethylene, nylon 11, polypropylene, polyethylene-lined EVA, and santoprene were all found to have maximum strain values that varied from the one day longitudinal strips ($p \leq 0.01$).

The elastic modulus values were found to be the same for ester-based polyurethane, ether-based polyurethane, EVA, polyethylene-lined EVA, santoprene, viton, neoprene, and silicone rubber ($p \leq 0.01$). Polyethylene, polypropylene and nylon 11 were found to have a different elastic modulus than the one day longitudinal strips. The results of all statistical t-tests performed are shown in Table 3.2.

3.1.4 Candidate Material/Blood Vessel Comparison (Circumferential)

The statistical analysis described in Section 2.2.5 was utilized to determine which candidate material is most similar in mechanical behavior to the aortic specimens cut in the circumferential direction. This study focused on the same mechanical properties of concern in the previous comparisons. The goal was to determine if any of the materials are statistically similar to all of the specified mechanical properties of the aortic tissue tested. This comparison also reaffirms if the direction of the testing has any effect on the properties obtained. The results were considered significant at the 0.01 level.

For the yield strength values neoprene and silicone rubber were found to have values that were statistically similar to the one day longitudinal strips ($p \leq 0.01$). Ester-based polyurethane, ether-based polyurethane, polyethylene, polypropylene, nylon 11, EVA, polyethylene-lined EVA, santoprene and viton were all found to have yield strength values that varied from the one day longitudinal strips ($p \leq 0.01$).

The elongation at yield was found to vary for ether-based polyurethane and neoprene ($p \leq 0.01$). Ester-based polyurethane, polyethylene, polypropylene, nylon 11, EVA, polyethylene-lined EVA, santoprene, viton, and silicone rubber were all found to have an elongation at yield that was statistically similar to the one day longitudinal strips ($p \leq 0.01$).

The elongation at break was found to be statistically similar for polypropylene, viton, neoprene, and silicone rubber ($p \leq 0.01$). Ester-based polyurethane, ether-based polyurethane, polyethylene, nylon 11, EVA, polyethylene-lined EVA and santoprene were all found to have an elongation at break that varied from the one day longitudinal strips ($p \leq 0.01$).

For the maximum stress values, ester-based polyurethane, ether-based polyurethane, polyethylene, polypropylene, EVA, polyethylene-lined EVA, and neoprene were all found to vary from the one day longitudinal strips ($p \leq 0.01$). Santoprene, viton, and silicone rubber were all found to have maximum stress values that were statistically similar to the one day longitudinal strips ($p \leq 0.01$).

For the maximum strain values, ether-based polyurethane, EVA, viton, neoprene, and silicone rubber were all found to be similar to the one day longitudinal strips ($p \leq 0.01$). Ester-based polyurethane, polyethylene, polypropylene, nylon 11, polyethylene-lined EVA, and santoprene were all found to have maximum strain values that varied from the one day longitudinal strips ($p \leq 0.01$).

The elastic modulus values were found to be the same for ester-based polyurethane, ether-based polyurethane, EVA, polyethylene-lined EVA, santoprene, viton, neoprene, and silicone rubber ($p \leq 0.01$). Polyethylene, polypropylene and nylon 11 were found to have an elastic modulus that varied from the one day longitudinal strips ($p \leq 0.01$). The results of all statistical t-tests are shown in Table 3.3.

Table 3.3: Results of Statistical t-Test for Circumferential Values ($p \leq 0.01$)

Material	Yield Strength (MPa)	Elongation at Yield (cm)	Elongation at Break (cm)	Stress Max (MPa)	Strain Max	Elastic Modulus (MPa)
Ester PU	fail	fail	fail	fail	fail	pass
Ether PU	fail	pass	fail	fail	pass	pass
LDPE	fail	pass	fail	fail	fail	fail
PP	fail	pass	pass	fail	fail	fail
Nylon 11	fail	pass	fail	fail	fail	fail
EVA	fail	pass	fail	fail	pass	pass
PE-EVA	fail	pass	fail	fail	fail	pass
Santoprene	fail	pass	fail	pass	fail	pass
Viton	fail	pass	pass	pass	pass	fail
Neoprene	pass	fail	pass	fail	pass	pass
Silicone	pass	pass	pass	pass	pass	pass

3.2 Discussion

The purpose of this study was to compare selected mechanical properties of canine blood vessel specimens and candidate modeling materials in order to determine the appropriate material to incorporate into a physical model of the abdominal aorta. One area of concern was to what degree did the mechanical properties of the blood vessels change with the amount of time that elapsed between extraction and testing. Another concern that needed to be addressed was whether or not the mechanical properties of the blood vessel test specimens varied with the direction in which they were cut from intact aortas. Once these areas were addressed it was then possible to choose an appropriate candidate material for future incorporation into an abdominal aortic model. The following sections discuss in detail the findings of this study.

3.2.1 Time Dependency of Arterial Tissue Properties

When studying the mechanical properties of blood vessels it is important to determine variations due to storage time before testing. Therefore, a comparison of the time-dependency of the vessels properties was performed. The three main properties of concern in this comparison were yield strength, maximum strain, and elastic modulus due to the fact that any amount of change in the vessel tissue properties over varying periods of testing would be expected to have the most significant effect on these specific properties.

The typical stress-strain plot of a blood vessel clearly demonstrates that this relationship begins with an extended period of small stress and then undergoes a sudden increase shortly after a strain value of approximately 1.5 has been reached.

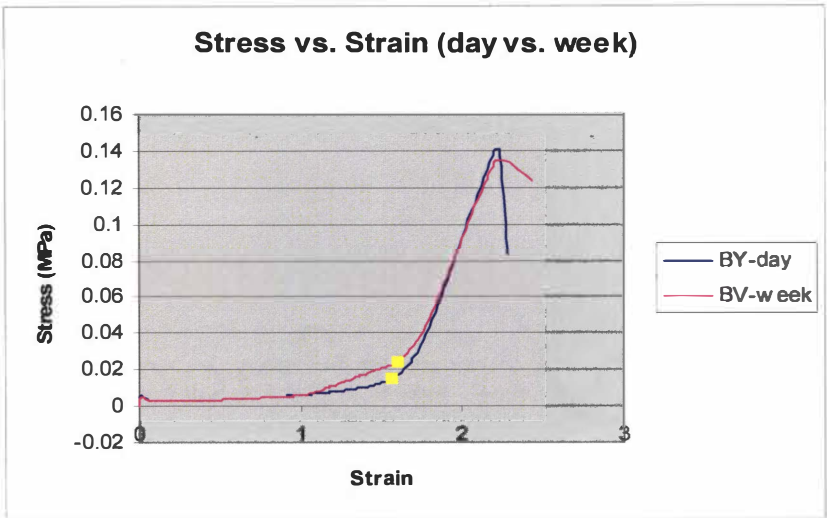

Figure 3.1: Stress-Strain Results (One day/ One week)

The value of strain at these points is highlighted in yellow on Figure 3.1. It was found that there was a 7.8% difference in these strain values for the day-old to week-old comparison and a 4.1% difference for the day-old to month-old comparison. These values help to verify that there is a strong similarity between all three samples that were tested. This increase signifies the point were the collagen components of the vessel start to bear the majority of the longitudinal force and is an indication of the stiffness of the vessel tissue. This area of a stress-strain curve for a typical blood vessel is known as the linear collagen region. The most significant mechanical properties of a blood vessel are derived from this part of the curve and are therefore of particular interest in this study.

Based on the plots presented in Figure 3.1 above and Figure 3.2 on page 39, as well as the statistical and percent difference analysis reported in Section 3.1.1, it was found that the mechanical properties of the vessels observed in this procedure were relatively unaffected by the amount of time between their extraction and when they were tested.

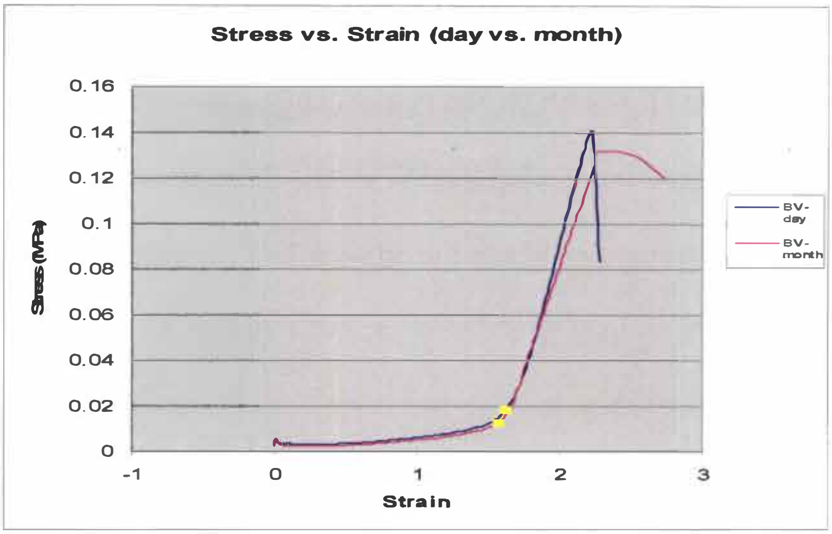

Figure 3.2: Stress-Strain Results (One Day/One month)

There is a strong similarity between the major mechanical properties including yield strength, maximum strain, and elastic modulus after one day, one week, and one month has elapsed. There is an especially strong similarity between the day-old and month-old samples in every property that was compared. A stronger similarity over a longer time suggests that the mechanical properties obtained are more a result of general variations in the population (e.g. larger breed, healthier canine) than the storage period. There are also similarities at the point were collagen begins to bear the longitudinal force. This is an indication that the tissue elements (e.g. elastin, collagen, etc.) responsible for the elasticity of the vessels remain unaffected by specimen storage for up to one month.

One reason that the selected mechanical properties remained relatively constant is that the vessels were stored in a saline-electrolytic solution. Storing the vessels in this solution kept them from drying which would have made the vessels brittle which in turn would cause the elastic modulus to increase (Fung 1995). The fact that they were refrigerated at approximately 40°F also helped prevent this effect on the vessels. Another possible explanation for this finding is that the vessels were stored for one month at the longest. It is safe to conclude that for this procedure the mechanical properties of the blood vessels tested were stable for up to a period of one month of storage.

3.2.2 Directional Dependency of Arterial Tissue Properties

Another comparison of interest is the differences between the results of uniaxial tensile tests of the tissue samples prepared in the longitudinal direction versus those prepared from circumferential strips of tissue. It has been shown in numerous studies that for vessels of varying position along the arterial tree the properties can vary when tested in different directions due to their anisotropic compositions (Wuyts *et al.* 1995). It was important to determine whether or not a significant difference in these properties occur in the vessels used in this study.

The only property that demonstrated any significant variation from the properties of the one day longitudinal strips was the maximum amount of stress which can be sustained. The value for maximum stress obtained from circumferential tests showed an increase of 20 kPa over the longitudinal values. This result was not unexpected since the lack of a systematic alignment of collagen fibers in the adventitia allows it to bear a larger amount of force in the circumferential direction once the vessel is subjected to a relatively high amount of strain ($L/L_0 \approx 1.0$-1.5)(Wuyts *et al.* 1995).

Based on the trends reflected in Figure 3.3 as well as the statistical and percent difference analysis reported in Section 3.1.2, it can be concluded that there is not a significant difference between the longitudinal values of the reported mechanical properties and those values obtained from circumferential testing.

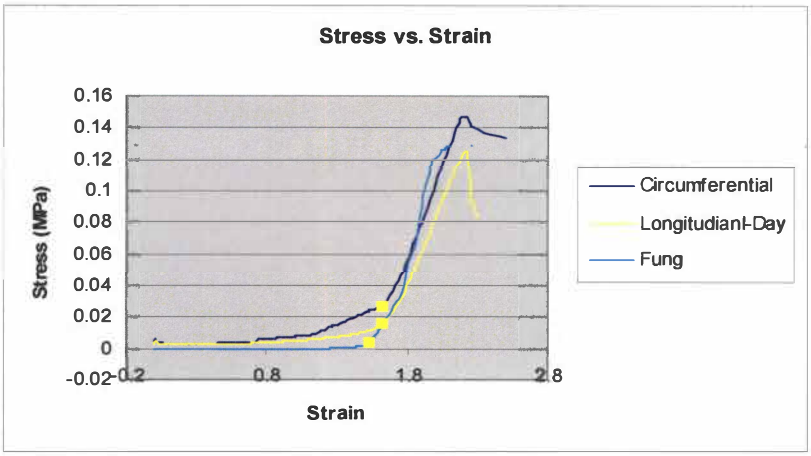

Figure 3.3: Stress –Strain Results (Circumferential/Longitudinal/Fung[1997])

In Figure 3.3 the point where the collagen starts to bear the load produced by the uniaxial tensile test is highlighted in yellow for each data plot. There is a strong similarity in the location of these points over a range of stress values from 20 to 40 kPa. This result was not surprising since collagen is known for bearing weight in the circumferential direction once the amount of strain has reached a critical point (Fung 1997).

The data plot presented in Figure 3.3 also illustrates tissue behavior similar to that reported by Fung after performing uniaxial tensile tests on post-mortem human abdominal aorta specimens (Fung 1997). The stress-strain curve provided by Fung shows a similarity to both the longitudinal and circumferential sample test curves obtained in this study. Fung's data shows the same initial zero stress state as the longitudinal and circumferential sample plots obtained in the present study. There is also a similarity in the point where collagen starts to bear the largest portion of the load. The curve produced from Fung's tests exhibits a smoother appearance than that of the longitudinal and circumferential test specimen graphs for the present study. This result is not surprising since the tissue samples tested for both the longitudinal and circumferential loading consisted of only three aortic specimens. A smoother plot of the stress-strain relationship in the present study would almost certainly occur if this procedure were altered to include samples of ten or more specimens which was not feasible due to limited availability of canine test specimens.

3.2.3 Material Selection for Abdominal Aorta Models

The statistical analysis reported in Sections 3.1.3 indicate that the candidate material whose mechanical properties best match that of a blood vessel tested in the longitudinal direction is silicone rubber. Silicone rubber shows a 10.2% difference in yield strength when compared to the day-old longitudinal sample. It shows an 11.6% difference in elongation at break when compared to the day-old longitudinal sample. The values for maximum strain show 11.4% difference. The elastic modulus of silicone rubber was shown be very similar to the one day longitudinal strip values with a difference of only 5.24%. The only major difference was with maximum stress which showed a difference of 21.7 % in comparison to the day-old longitudinally tested sample.

The statistical analysis reported in Sections 3.1.4 indicates that the candidate material whose mechanical properties most resemble that of a blood vessel tested in the circumferential direction is silicone rubber. Silicone rubber shows a 9.3% difference in yield strength when compared to the circumferential sample. It shows a 10.3% difference in elongation at break when compared to circumferential sample. The values for maximum strain show 10.2% difference. The elastic modulus of silicone rubber was shown to be very similar to the circumferential sample with a difference of 6.1%. The only major difference was with maximum stress which showed a difference of 21.2 % when compared to the circumferentially tested sample.

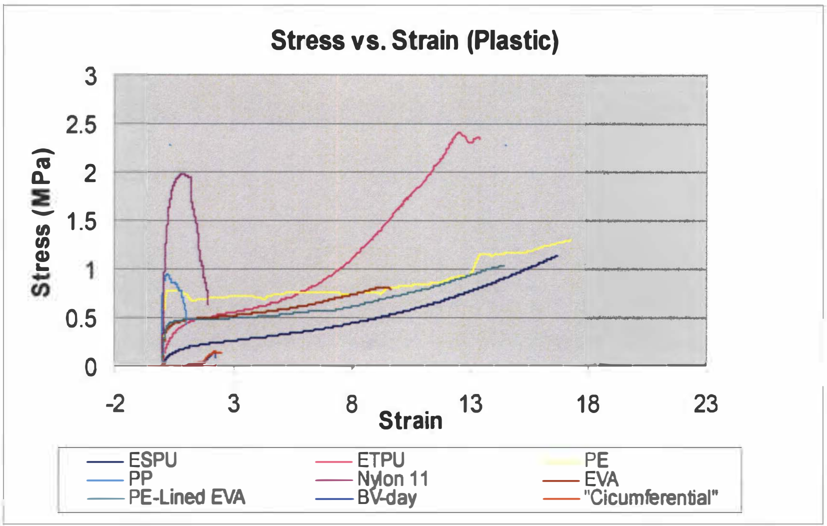

Figure 3.4: Stress-Strain Results (Plastic)

A prime objective of this investigation was to determine which of the selected candidate materials is the most similar in mechanical behavior to the arterial tissue. The stress-strain relationships for the candidate materials tested are shown in Figure 3.4 above and Figure 3.5 on page 44. The data plot shown in Figure 3.4 clearly demonstrates that none of the selected plastics have similar mechanical properties to those seen in the canine specimens. This is concluded from observing that the stress and strain values for all of the plastics are much higher than those seen in the blood vessels.

Figure 3.5 on the other hand shows a similarity in the elastic regions of both santoprene and silicone rubber. Silicone rubber was the only polymer tested that passed the t-test for all values of the mechanical properties reported which indicates a statistical similarity in all of the mechanical properties evaluated. It can also be seen that the differences for both longitudinal and circumferential uniaxial testing are minimal, especially with the elastic modulus values reported. This property is highly important since it demonstrates the flexibility or rigidity of a material..

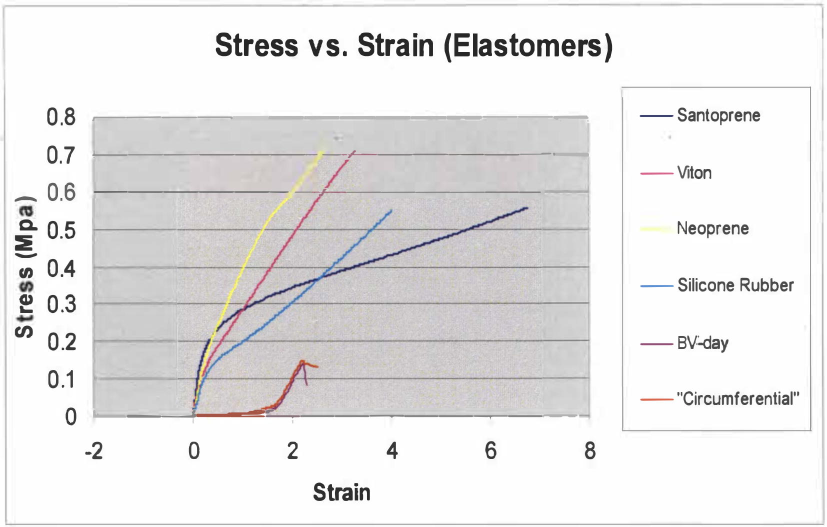

Figure 3.5: Stress-Strain Results (Elastomers)

It is apparent from Figure 3.5 and the percent difference analysis that the values for the elongation at yield in both the longitudinal and circumferential samples of arterial tissue are much larger than those for silicone rubber. Such a large difference is a result of elastin in vascular tissue bearing the majority of the load at lower strains. Since silicone rubber is a relatively homogenous material it doesn't experience the initial extended small stress seen in the blood vessels.

Some reasons for the differences that are seen between the candidate materials and arterial tissue are human error and possible deficiencies in the testing procedure. The sudden drop at the termination point of the stress-strain curves for all arterial tissue samples indicates that slipping may have occurred at the end of the test run. This in turn would cause small deviations from the properties seen in the candidate materials and those in the arterial tissue samples. Also, anytime large amounts of data are being interpreted there is a chance that the values may be evaluated incorrectly which would cause false differences or similarities to be observed.

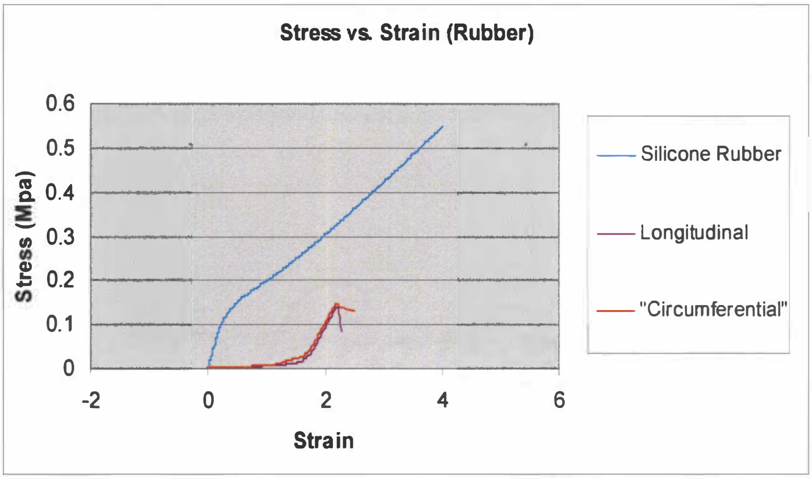

Figure 3.6: Stress-Strain Results (Silicone Rubber)

Figure 3.6 demonstrates a similarity between the longitudinal, circumferential, and the silicone rubber samples. The initial increase in stress shown for silicone rubber is almost identical to the increase shown in both the longitudinal and circumferential blood vessels at a relative strain of approximately 1.5 to 1.8. The initial small stress period shown in the blood vessels is a reflection of the elastin composition of the vessels and is not present with silicone rubber due to its homogenous composition. Since collagen bears the majority of both longitudinal and circumferential load, the initial small stress seen in the vessels was ignored for this part of the present investigation. Such a close similarity in the mechanical properties is the principal basis for the conclusion that silicone rubber the candidate material most similar to a blood vessel in terms of mechanical properties.

Chapter 4

Conclusions and Recommendations

4.1 Conclusions

The results from this study provide a useful basis for the design of a physical model of the abdominal aorta with an emphasis being placed on the mechanical properties of the chosen material. There is a strong correlation seen in the time dependency comparison as well as the longitudinal to circumferential mechanical properties comparison. The material selection process led to the decision for silicone rubber as the material to incorporate into a physical model of the abdominal aorta.

Results from the time dependency comparison show a strong similarity between the different samples of canine aorta specimens. There was an especially strong similarity in the mechanical properties of the one day and one month longitudinal samples which led to the conclusion that the mechanical properties of these vessels were not altered to a point that would affect the outcome of material selection. It was also apparent that the strain value where collagen starts to bear the applied load was nearly identical in all of the samples tested. This demonstrated that the overall elasticity of the specimens was unaffected by the period of storage up to one month. These findings demonstrated consistency in the measured mechanical properties of the arterial tissue and supported the results of the material selection process.

Results from the directional dependency comparison showed there was no significant difference in the mechanical properties of the canine aorta specimens when tested on longitudinally or circumferentially cut specimens. There was a close match in the values of yield strength, maximum strain, and the elastic modulus which are the most important to consider since any degradation of the vessels would most likely be reflected in these changes in these properties. There was an especially strong similarity in the maximum strain as well as the amount of stress present when strains are such that collagen starts to bear a large fraction of the applied load. This observation led to the conclusion that the overall elasticity of the vessels tested was consistent when the load was applied to arterial tissues that cut longitudinally and circumferentially.

The results in the material selection process led to the conclusion that silicone rubber had the most similar mechanical properties of the all candidate materials tested and therefore should be incorporated into an abdominal aorta model. Silicone rubber was the only polymer tested that passed the student t-test for all values. The percent differences between the one day longitudinal strips and the silicone rubber samples were minimal for most values, especially with the elastic modulus values reported for the material. The initial increase in stress shown for silicone rubber was almost identical to the increase shown in the blood vessels at a relative strain of approximately 1.6. It was apparent from the data plots and the percent difference analysis that the values for maximum stress are somewhat larger for the silicone rubber. This finding did not affect the results of the comparison since blood vessels normally do not experience large amounts of longitudinal stress or strain in a physiological setting.

In conclusion, this study produced an effective material selection process for designing a physical model of the abdominal aorta. Although silicone rubber has very similar properties, in future studies a wider variety of materials should be tested in order to ensure the best available material are being utilized. In the future advanced testing procedures as well as advanced production processes will lead to a sufficient model of the abdominal aorta from which observations of blood flow properties can be effectively conducted.

4.2 Recommendations for Future Work

The future development of a mechanically-matched abdominal aorta model should include but not be limited to the following considerations. Testing should be expanded to include biaxial tests of not only the vessels but the polymers as well since it will provide an insight into the behavior of the vessels when loads are applied in two directions at once. The testing procedure should incorporate different materials including various stent graft materials or various types of polymers metal blends. It would also be useful to test human aortas in order to study individual donor mechanical property variations and ensure that the most human-like comparison can be made. Incorporating the mathematical representation of the stress-strain relationship and comparing it to the results of the testing could provide another validation to the testing method and therefore should be utilized.

The future construction of a prototype will need to utilize methods such as those described in Appendix B. An effective approach is expected to involve stereolithography due to its ability to construct complex geometries. Once a successful trunk model has been constructed, then it will be necessary to add the iliac bifurcations to the prototype. Adding this to the process will most likely prove to be difficult and in all likelihood will also require stereolithography to be accomplished. Once the iliac bifurcation is added then the remaining branches will need to be incorporated by utilizing the same method that produced the trunk and the iliac arteries. The varying thickness of blood vessels plays a significant role in the overall properties that are observed and will need to be incorporated in future studies. It also might prove to be beneficial if a layered model can be produced with different materials that mimic the properties of each layer.

Bibliography

Bibliography

Bargeron, B, G. Hutchins, G. W. Moore, O. Deters, F. Mark, and M. Friedman (1985). "Distribution of the Geometric Parameters of Human Aortic Bifurcations" *Applied Physics Laboratory and the Department of Pathology, John Hopkins University*, 109-113.

Caro, C., T. Pedley, R. Schroter, and W. A. Seed (1978). "The Mechanics of the Circulation" *Oxford University Press,* New York .

Chandran, K. (2001). "Flow Dynamics in the Human Aorta: Techniques and Applications" *University of Iowa.*

Dawson, T. (1991). "Engineering Design of the Cardiovascular System of Mammals" *Prentice Hall,* Englewood Cliffs, New Jersey.

Degroot, M. (2002). "BiomechanicsProbability and Statistics" (3rd ed.) *Addison-Wesley,* New York.

Dobrin, P. (1978). "Mechanical Properties of Arteries" *Physiological Reviews,* 58 397-497.

Feldman, D. and A. Barbalata (1996). "Synthetic Polymers: Technology, Properties, and Applications" *Chaoman and Hall,* New York.

Fung, Y. C. (1997). "Biomechanics: Mechanical Properties of Living Tissues" (2nd ed.) *Springer-Verlag,* New York.

Fung, Y. C. (1997). "Biomechanics: Circulation" (2nd ed.) *Springer-Verlag,* New York.

Fung, Y. C. and S. Q Liu (1995). "Determination of the Mechanical Properties of the Different Layers of Blood Vessels *In Vivo" Proctor National Academic Science,* 92, 2169-2173.

Gray, H. (1918). "Anatomy of the Human Body" Lea & Febiger, Philadelphia, 1918; Bartleby.com, 2000.

Hensley, A. (2001). "Analytical and Computational Model for Aortic Hemodynamics Accountinf for aortic Elasticity and Arterial Branch Flow Effects" Masters Thesis, University of Tennessee, Knoxville.

Järvisalo, M., L. Jartti, K. Näntö-Salonen, K. Irjala, T. Rönnemaa, J. Hartiala, D. Celermajer, and O. Raitakari, (2001). "Increased Aortic Intima-Media Thickness" *Circulation*, 104, 2943.

Kuecherer, H. F., A. Just, and H. Kirchheim (2000). "Evaluation of Aortic Compliance in Humans" *American Journal of Heart Circulation Physiology*, 278, 1411-1413.

Lee, D. and J. Y. Yen (2002). "Numerical Simulation of Steady Flow Fields in a Model of Abdominal Aorta with its Peripheral Branches" *Journal of Biomechanics*, 35, 1115-1122.

Levick, J. R. (2003). "An Introduction to Cardiovascular Physiology" (4th ed.) *Arnold,* London, England.

Li, J. K. (2004), "Dynamics of the Vascular System: Series on Bioengineering and Biomedical Engineering" (1st Ed.) *World-Scientific Publishing* London

Liepsch, D.W. (1986). "Flow in Tubes and Arteries: A Comparison" *Biorheology*, 23, 395-433.

Monson, K. (2001). "Mechanical and Failure Properties of Human Cerebral Blood Vessels" Ph. D. Dissertation, University of California, Berkeley.

Nikuradse, J. (1981). "Law of Flow in Rough Pipes" *Technical Memorandum 1292. National Advisory Committee for Aeronautics.*

Poutanen, T., T. Tikanoja, H. Sairanen, and E. Jokinen (2003). "Normal Aortic Dimensions and Flow in 168 Children and Young Adults" *Clinical Physiology Functional Imaging*, 23, 224-229.

Schulze-Bauer, P., and G. Holzapfel (2002). "Mechanics of the Human Femoral Adventitia Including the High Pressure Response" *American Journal of Heart Circulation Physiology*, 282, 2427-2440.

Schvartzman, P., F. Fuchs, A. Mellos, M. Coli, M. Schvartzman, and L. Moreira (2002). "Normal Values of Endocardiographic Measurements; A Population-Based Study" *Arq. Brasil Cardioology*, 75, 111-114.

Segers, P., F. Dubois, D. De Wachter, and P. Verdonck (1998) "Role and Relevancy of a Cardiovascular Simulator" *Journal for Extracorporeal Circulation, Assist Devices, Transplantation and Artificial Organs* 3 (1): 48-56.

Silver, F., P. Snowhill, and D. Foran (2003). "Mechanical Behavior of Vessel Wall: A Comparative Study of Aorta, Vena Cava, and Carotid Artery" *Annals of Biomedical Engineering*, 31, 793-803.

Spence, A. P. and E. B. Mason (1987) 'Human Anatomy and Physiology" (3^{rd} ed.) The Benjamin/Cummings Publishing Company, Inc.

Summers, R, J. Andrasko-Burgois, I. Furstein, S. Hill, E. Jones, M. Busse, B. Wise, K. Bove, B. Rishforth, E. Tucker, T. Spray, and J. Hoag (1998). "Evaluation of the Aortic Root by MRI: Insights from Patients with Homozygous Familial Hypercholestorolemia" *Circulation*, 98, 509-518.

Wuyts, F., V. Vanhuyse, G. Langewouters, W. Decraemer, E. Raman, and S. Buyle (1995). "Elastic Properties of Human Aortas in Relation to Age and Atherosclerosis: A Structural Model" *Physiology and Medical Biology*, 40, 1577-1597.

Zulliger, M., P. Fridez, K. Hayashi, and N. Stergiopoulos (2004). "A Strain Energy Function for Arteries Accounting for Wall Composition and Structure" *Journal of Biomechanics*, 37, 989-1000.

Appendix

Appendix A

Model Specifications

When designing a model of the abdominal aorta it is important to pay close attention to the varying geometry of the arterial system. The arterial system can best be described as a tapered branching system. In a normal arterial system, the branching vessels tend to be narrower than the trunk vessel but have a larger cross sectional area. This means the ratio of cross-sectional area of the branching vessels to that of the trunk vessel tends to be greater than 1.0 which in turn has a significant effect on pulsatile energy transmission. In general, the thickness of the artery tends to decrease in the descending direction but for the initial model the thickness will be taken as a constant. The value of this thickness as well as the average diameters of the abdominal aorta and iliac arteries is given in Table A1.

Table A1: Dimensions for Use in Design of Aorta Model

Vessel Thickness (mm)	1.5
Abdominal Aorta Insertion Diameter (cm)	1.85
Abdominal Aorta Endpoint Diameter (cm)	1.75
Iliac (Right and Left) Insertion Diameter (cm)	1.72
Iliac (Right and Left) Endpoint Diameter (cm)	1.35

Values for the internal diameters of the ascending aorta, abdominal aorta, femoral artery, and arteriole have shown a significant taper from the root of the aorta to the aorto-iliac junction. This combined with branching that occurs is the main cause of an overall non-uniformity that it observed throughout the system. The taper that occurs in the abdominal aorta is close to an exponential form and can be written as:

$$A(x) = A_{in} e^{-kx}$$

where **A(x)** is the cross-sectional area along the abdominal aorta, $\mathbf{A_{in}}$ is the cross-sectional area at the insertion point of the abdominal aorta, **x** is the position along the abdominal aorta, and **k** is a constant known as the geometric taper factor. This taper factor is known to vary significantly with different vasoactive conditions as well as in pathological conditions. The negative sign in the exponential term of the equation denotes that the area decreases along the path. Overall changes in the anatomical area with position along the abdominal aorta are represented in Figure A1. A derivation of the geometric taper factor of this model based on the dimensions in Table A1 is given in Appendix C.

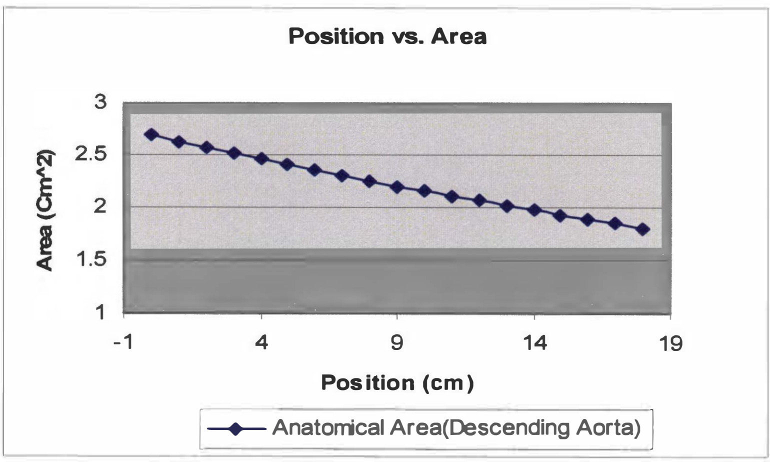

Figure A1: Change in Anatomical Area along the Abdominal Aorta

A computer-aided drawing of the basic design for the model is shown in Figure A2(A-C). The drawings provide an illustration of the objective of this design although the taper of the model is not represented effectively. A basic hand drawing depicting the taper of the model as well as the angle of the iliac bifurcation is shown below. The goal is to eventually construct a model based on such drawings.

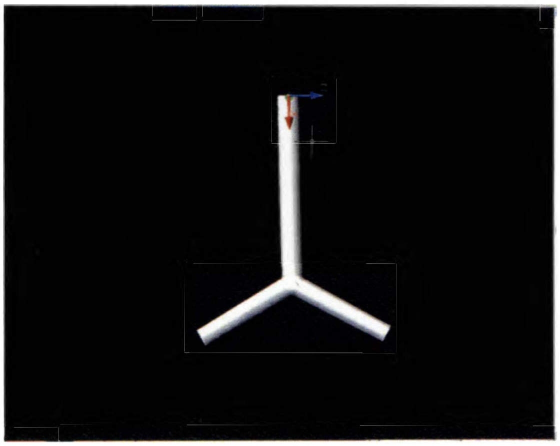

A) Frontal view AutoCAD Model

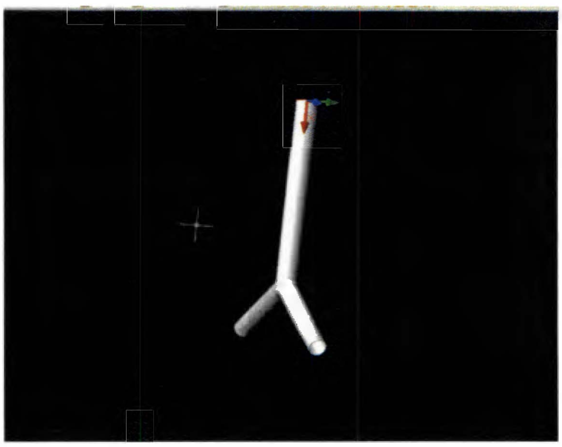

B) Angled view AutoCAD Model

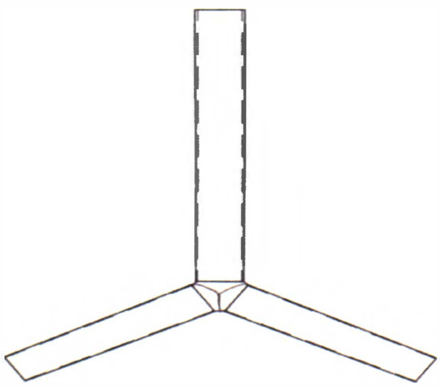

C) Preliminary AutoCAD Drawing

Figure A2: Computer-Aided Model Drawings

Appendix B

Preliminary Ideas for Future Model Production

Injection Molding

Injection Molding is a manufacturing process that involves forcing melted plastic in to a mold cavity. Once the plastic has cooled the part is ejected from the mold. Injection molding is often used in mass-production and prototyping. It is one of the most common manufacturing processes utilized in producing a wide variety of polymers.

There are many reasons that injection molding should be utilized to produce this model. Among these are that high tolerances are repeatable in the process which would allow for a prototype with accurate dimensions. Another advantage is that a wide range of materials could be used which would be useful if the silicone rubber needed to be reinforced in some way to improve mechanical characteristics. Some disadvantages of utilizing injection molding are that the equipment needed can be expensive, running costs are usually high and the mold needed would be difficult and expensive to create.

Rotational Injection Molding

Rotational injection molding is a special form of injection molding that is used for manufacturing hollow plastic products. It consists of introducing a known amount of plastic in powder, granular, or liquid form into a hollow, shell-like mold. The mold is heated and simultaneously rotated about two principle axis so that the plastic enclosed in the mold adheres to and forms a layer against the mold surface. When the plastic is rigid enough, the mold rotation is stopped to allow the removal of the plastic product from the mold.

Rotational molding could prove useful for a number of reasons. It produces a nearly stress-free part which means the model produced would have accurate dimensions and a smooth inner surface. Rotational molds have the ability to produce accurate as well as varying wall thicknesses which would be extremely beneficial to this model. Rotational molds are also relatively inexpensive to fabricate which gives it a major advantage over regular injection molding. The main disadvantage of rotational molding is that the apparatus utilized can be expensive and has a tendency to malfunction on a regular basis.

Stereolithography

Stereolithography is also known as 3D Layering and 3D Printing. It is the process of turning CAD designs into real 3D objects in a matter of hours. Stereolithography goes straight from design to the prototype. It is a manufacturing process that uses a UV laser to create successive cross-sections of a 3D object within a vat of a specific liquid polymer. A platform is placed on top of the vat filled with the polymer. The platform is then moved to a point just below the surface of the resin. As the solid state UV laser traces the layer in the polymer, the resin begins to cure; solidifying the part to be manufactured.

The stereolithography process consists of the following steps. First, a 3-D model is created using CAD software. Next, software slices up the CAD model into about 5-10 layers millimeter. Once this is completed, the platform drops down into the tank layer by layer until the model is completed. The 3-D object designed with CAD software has to be modified to add supports to raise it off of the platform slightly. Once the process is complete, the platform is raised out of the polymer and the 3D model is rinsed in a solvent and baked in an ultra-violet oven to completely cure the plastic.

There are many advantages to utilizing stereolithography in the production of this model. One is that the CAD drawings necessary for the production have already been produced. Another is that when compared to the previous methods, stereolithography is much more capable of producing the complex geometry that this model presents. Stereolithography is also inexpensive when compared to the previous methods and does not require a mold which would cut down on the amount of finishing that is necessary.

Appendix C

Statistical Analysis

Time Dependency Comparison

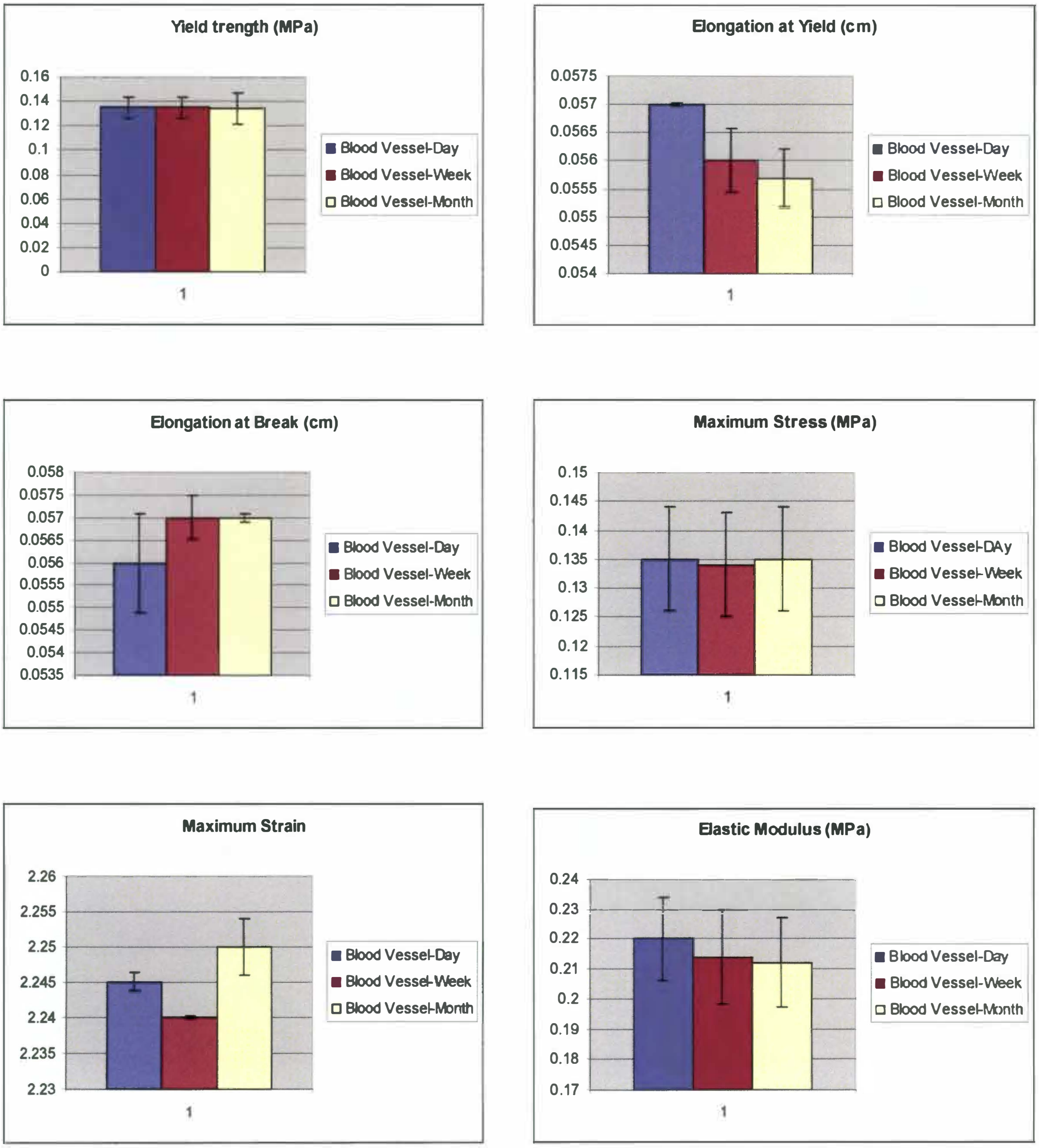

FigureC1: Statistical Comparison: Time Dependency

Polymer/Blood Vessel Comparison (Longitudinal)

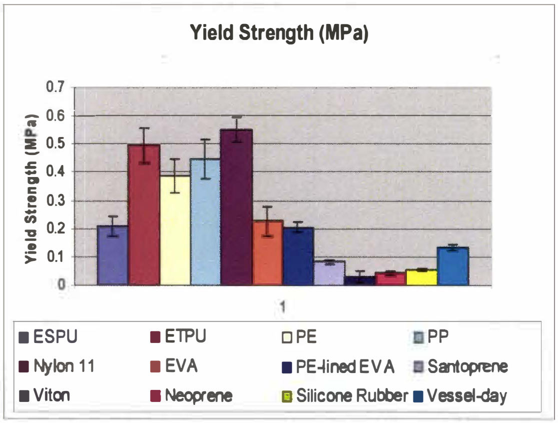

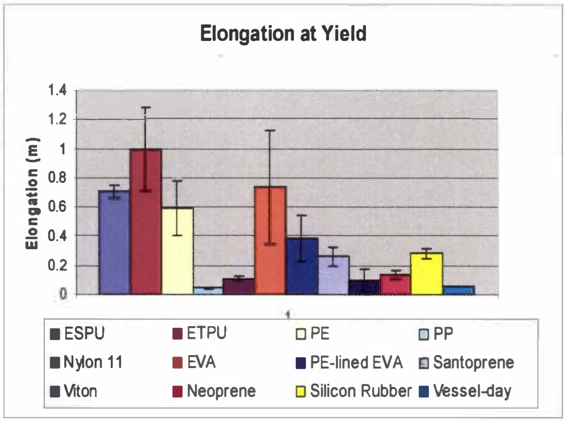

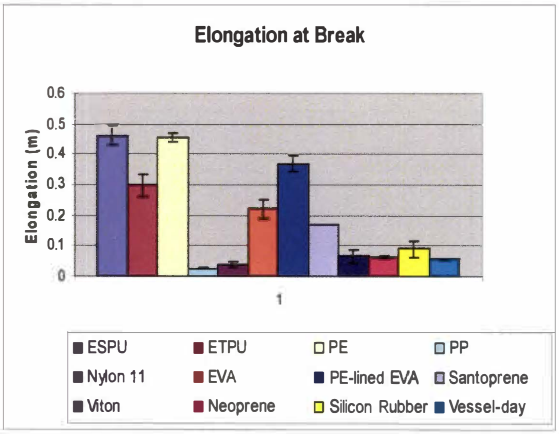

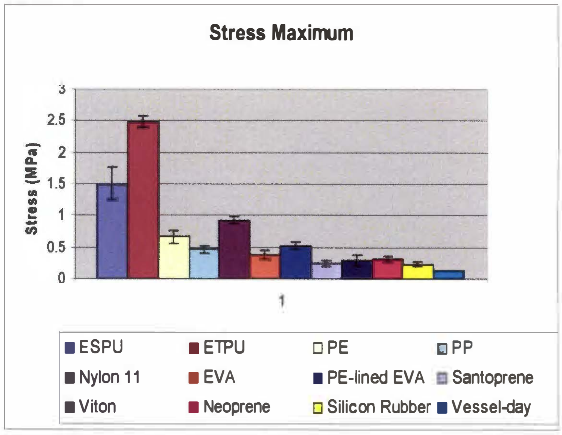

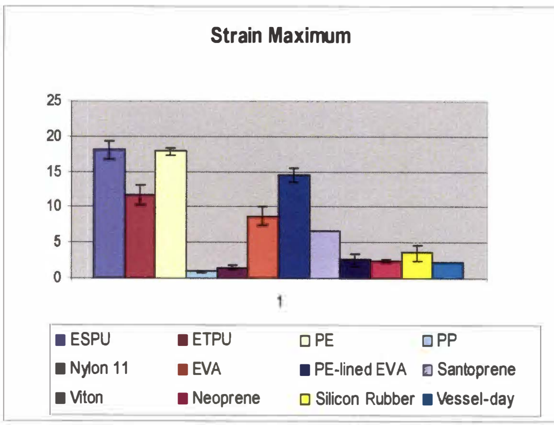

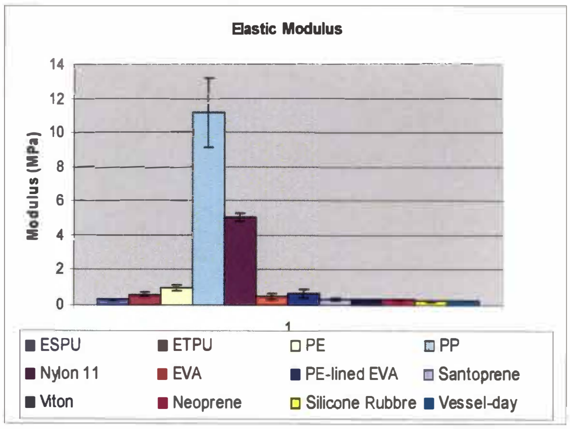

Figure C2: Statistical Comparison: Longitudinal Sample

Polymer/Blood Vessel Comparison (Circumferential)

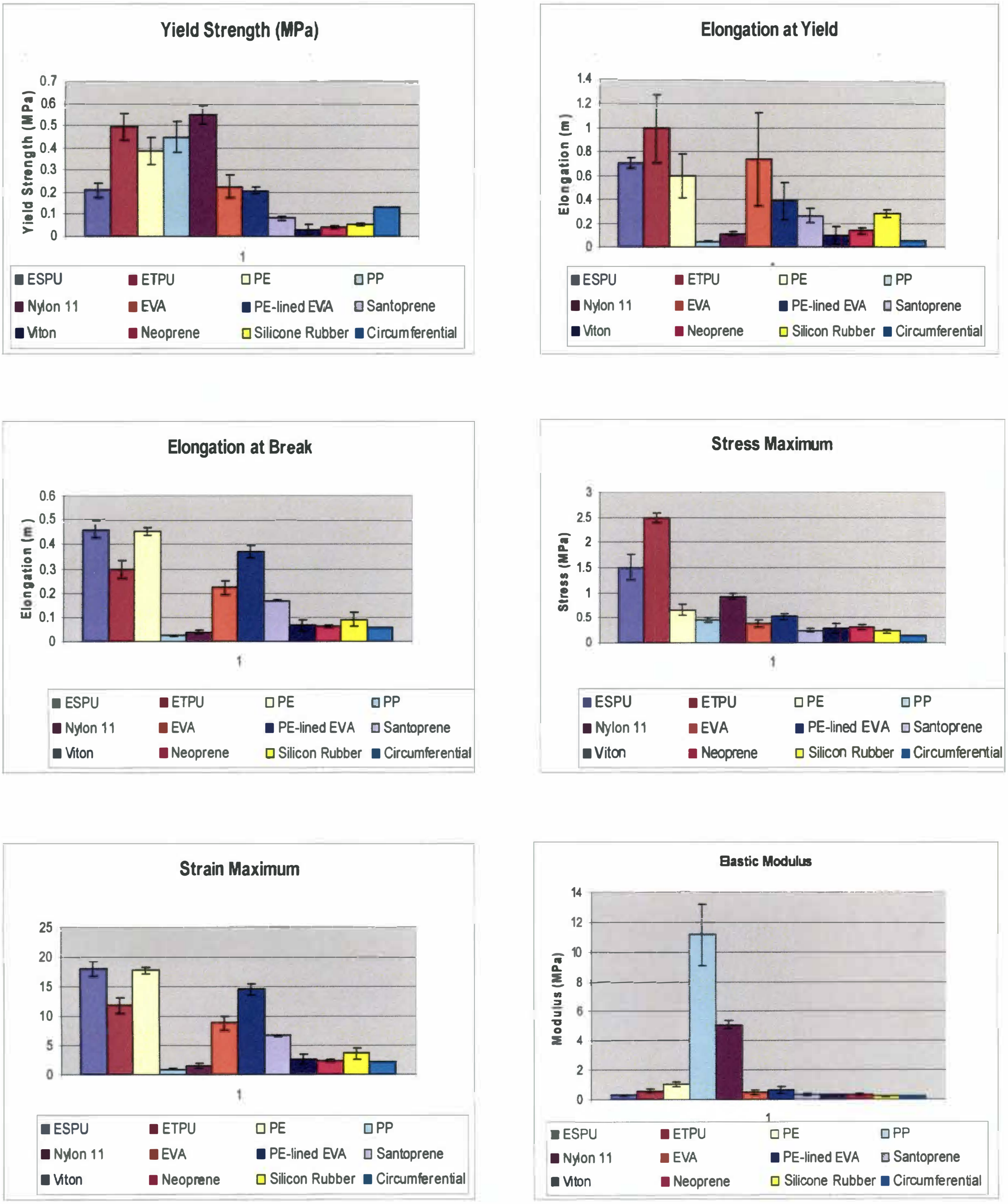

Figure C3: Statistical Comparison: Circumferential Sample

Appendix D

Calculation of the Taper Factor of the Abdominal Aorta

According to Caro, the change in the abdominal aorta due to tapering fits the exponential equation of the form:

$$A(x) = A_{in} e^{-kx}$$

where A_{in} is the initial area of the vessel, x is the position along the vessel and k is the taper factor. Therefore, at the exit of the abdominal aorta:

$$\frac{A_{out}}{A_{in}} = e^{-kx}$$

Taking the natural logarithm of both sides' yields:

$$\ln\left(\frac{A_{out}}{A_{in}}\right) = -kx$$

Solving for the taper factor k gives the following equation:

$$k = -\frac{1}{x}\ln\left(\frac{A_{out}}{A_{in}}\right)$$

Using values for the inlet and outlet diameter given in Table A1 where D_{in} = 1.85 cm and D_{out} = 1.75 cm, Equation yields a value for taper factor of k= 0.585 m^{-1}.

Vita

Benjamin Michael Lamie was born in Johnson City, TN, on January 31st 1981. He attended Unicoi County High School and graduated in May 1999. He attended East Tennessee State University where he studied pre-medicine. After changing his major to engineering he enrolled at the University of Tennessee, Knoxville, in Fall 2001. He received the degree of Bachelor of Science in Biomedical Engineering in May 2004. He continued his education at UTK earning the degree of Master of Science in Engineering Science in December 2005.